

REPORT DOCUMENTATION PAGE

Form Approved OMB NO. 0704-0188

Public Reporting Burden for this collection of information is estimated to average 1 hour per response, including the time for reviewing instructions, searching existing data sources, gathering and maintaining the data needed, and completing and reviewing the collection of information. Send comment regarding this burden estimate or any other aspect of this collection of information, including suggestions for reducing this burden, to Washington Headquarters Services, Directorate for Information Operations and Reports, 1215 Jefferson Davis Highway, Suite 1204, Arlington VA, 22202-4302, and to the Office of Management and Budget, Paperwork Reduction Project (0704-0188), Washington DC 20503

1. AGENCY USE ONLY (Leave Blank)		2. REPORT DATE: 19-Jul-2007	3. REPORT TYPE AND DATES COVERED Final Report 1-Jun-2004 - 31-May-2007	
4. TITLE AND SUBTITLE Autoignition and Combustion of Diesel and JP-8			5. FUNDING NUMBERS W911NF-04-1-0139	
6. AUTHORS Kalyanasundaram Seshadri			8. PERFORMING ORGANIZATION REPORT NUMBER	
7. PERFORMING ORGANIZATION NAMES AND ADDRESSES University of California - San Diego Office of Contract & Grant Administration 9500 Gilman Drive, Mail Code 0934 La Jolla, CA 92093 -0934				
9. SPONSORING/MONITORING AGENCY NAME(S) AND ADDRESS(ES) U.S. Army Research Office P.O. Box 12211 Research Triangle Park, NC 27709-2211			10. SPONSORING / MONITORING AGENCY REPORT NUMBER 45241-EG.2	
11. SUPPLEMENTARY NOTES The views, opinions and/or findings contained in this report are those of the author(s) and should not be construed as an official Department of the Army position, policy or decision, unless so designated by other documentation.				
12. DISTRIBUTION AVAILABILITY STATEMENT Distribution authorized to U.S. Government Agencies Only, Contains Proprietary			12b. DISTRIBUTION CODE	
13. ABSTRACT (Maximum 200 words) The abstract is below since many authors do not follow the 200 word limit				
14. SUBJECT TERMS Autoignition, Surrogate Fuels, JP-8			15. NUMBER OF PAGES Unknown due to possible attachments	
			16. PRICE CODE	
17. SECURITY CLASSIFICATION OF REPORT UNCLASSIFIED	18. SECURITY CLASSIFICATION ON THIS PAGE UNCLASSIFIED	19. SECURITY CLASSIFICATION OF ABSTRACT UNCLASSIFIED	20. LIMITATION OF ABSTRACT UL	

Report Title

Autoignition and Combustion of Diesel and JP-8

ABSTRACT

The Department of Defense directive 4140.25 dated April 12, 2004 mandates that "primary fuel support for land-based air and ground forces in all theaters shall be accomplished using a single kerosene-based fuel, in order of precedence: JP-8, commercial jet fuel (with additive package), or commercial jet fuel (without additives)." The objective of the proposed research is to understand those key aspects of combustion of JP-8 that are required to facilitate this conversion. It has been established that a useful approach to understanding combustion of JP-8 is to first develop surrogates that reproduce selected aspects of combustion of JP-8. Experimental, numerical and analytical studies have been carried out. The Aachen surrogate made up of n-decane (80 %) and trimethylbenzene (20 %) by liquid volume, and the UCSD surrogate made up of n-dodecane (60 %), methylcyclohexane (20 %), and o-xylene (20 %) by liquid volume were found to best reproduce autoignition and extinction characteristics of JP-8.

List of papers submitted or published that acknowledge ARO support during this reporting period. List the papers, including journal references, in the following categories:

(a) Papers published in peer-reviewed journals (N/A for none)

(1) Seshadri, K., "Chemical Inhibition of Nonpremixed Methane Flames by CF₃Br", Combustion Science and Technology, Volume 177, 2005, pp 871-906.

(2) Seshadri, K., Peters, N., and Paczko, G., "Rate-Ratio Asymptotic Analysis of Autoignition of n-Heptane in Laminar Nonpremixed Flows", Combustion and Flame, Volume 146, 2006, pp 131-141.

(3) Humer, S., Frassoldati, A., Granata, S., Faravelli, T., Ranzi, E., Seiser, R., and Seshadri, K., "Experimental and Kinetic Modeling Study of Combustion of JP-8, its Surrogates and Reference Components in Laminar Nonpremixed Flows", Proceedings of the Combustion Institute, Volume 31, 2007, pp 393-400.

(4) Seiser, R., Humer, S., Seshadri, K., and Pucher, E., "Experimental Investigation of Methanol and Ethanol Flames in Nonuniform Flows", Proceedings of the Combustion Institute, Volume 31, 2007, pp 1173-1180.

(5) Seshadri, K., and Bai, X. S., "Rate-Ratio Asymptotic Analysis of the Structure and Extinction of Partially Premixed Flames", Proceedings of the Combustion Institute, Volume 31, 2007, pp 1181-1188.

Number of Papers published in peer-reviewed journals: 5.00

(b) Papers published in non-peer-reviewed journals or in conference proceedings (N/A for none)

Number of Papers published in non peer-reviewed journals: 0.00

(c) Presentations

Number of Presentations: 0.00

Non Peer-Reviewed Conference Proceeding publications (other than abstracts):

(1) Lee, J., Humer, S., Seiser, R., Seshadri, K., and Pucher, E., "The Structure of Nonpremixed Toluene Flames," Paper 04S-17, Western States Section of the Combustion Institute, 2004 Spring Meeting, University of California at Davis, March 29-30, 2004.

(2) Humer, S., Seiser, R., and Seshadri, K., "Extinction and Autoignition of Liquid Hydrocarbon Fuels Under Nonpremixed Conditions: Asymptotic Theory with Comparison to Experiment," Paper 04S-56, Western States Section of the Combustion Institute, 2004 Spring Meeting, University of California at Davis, March 29-30, 2004.

(3) Niemann, U., Aerts, J. A. H., Humer, S., and Seshadri, K., "Extinction of Methanol Flames in Premixed Flows," Paper 06S-05, 2006 Spring Meeting, Western States Section of the Combustion Institute, University of Idaho, March 27-28, 2006.

(4) Seshadri, K., Peters, N., and Paczko, G., "Rate-Ratio Asymptotic Analysis of Autoignition of n-Heptane in Laminar Nonpremixed Flows," Paper 06S-30, 2006 Spring Meeting, Western States Section of the Combustion Institute, University of Idaho, March 27-28, 2006.

(5) Humer, S., Frassoldati, A., Granata, S., Faravelli, T., Ranzi, E., Seiser, R., and Seshadri, K., "Experimental and Kinetic Modeling Study of Combustion of JP-8, its Surrogates and Reference Components in Laminar Nonpremixed Flows," Paper 06S-41, 2006 Spring Meeting, Western States Section of the Combustion Institute, University of Idaho, March 27-28, 2006.

(6) Humer, S., Seshadri, K., and Seiser, R., "Combustion of Jet Fuels and its Surrogates in Laminar Nonuniform Flows," Paper E09, The 5th U. S. Combustion Meeting, University of California at San Diego, March 25-28, 2007.

(7) Niemann, U., Gerritzen, J., Seiser, R., Humer, S., and Seshadri, K., "Autoignition and extinction of Methyl-Esters in Non-Premixed Flows," Paper # A17, The 5th U. S. Combustion Meeting, University of California at San Diego, March 25--28, 2007.

(8) Gerritzen, J., Aerts, J., Humer, S., and Seshadri, K., "Extinction of Premixed Methanol and Ethanol Flames in Counterflow," Paper # A31, The 5th U. S. Combustion Meeting, University of California at San Diego, March 25-28, 2007.

Number of Non Peer-Reviewed Conference Proceeding publications (other than abstracts): 8

Peer-Reviewed Conference Proceeding publications (other than abstracts):

Number of Peer-Reviewed Conference Proceeding publications (other than abstracts): 0

(d) Manuscripts

Seshadri, K., Humer, S., and Seiser, R., "Activation-Energy Asymptotic Theory of Autoignition of Condensed Hydrocarbon Fuels in Nonpremixed Flows with Comparison to Experiment," Submitted for publication in Combustion Theory and Modelling, June 2007.

Number of Manuscripts: 1.00

Number of Inventions:

Graduate Students

<u>NAME</u>	<u>PERCENT SUPPORTED</u>
Maria Petrova	0.49
Priyank Saxena	0.37
FTE Equivalent:	0.86
Total Number:	2

Names of Post Doctorates

<u>NAME</u>	<u>PERCENT SUPPORTED</u>
FTE Equivalent:	
Total Number:	

Names of Faculty Supported

<u>NAME</u>	<u>PERCENT SUPPORTED</u>	National Academy Member
Kalyanasundaram Seshadri	0.61	No
FTE Equivalent:	0.61	
Total Number:	1	

Names of Under Graduate students supported

<u>NAME</u>	<u>PERCENT SUPPORTED</u>
FTE Equivalent:	
Total Number:	

Student Metrics

This section only applies to graduating undergraduates supported by this agreement in this reporting period

- The number of undergraduates funded by this agreement who graduated during this period: 0.00
- The number of undergraduates funded by this agreement who graduated during this period with a degree in science, mathematics, engineering, or technology fields:..... 0.00
- The number of undergraduates funded by your agreement who graduated during this period and will continue to pursue a graduate or Ph.D. degree in science, mathematics, engineering, or technology fields:..... 0.00
- Number of graduating undergraduates who achieved a 3.5 GPA to 4.0 (4.0 max scale):..... 0.00
- Number of graduating undergraduates funded by a DoD funded Center of Excellence grant for Education, Research and Engineering:..... 0.00
- The number of undergraduates funded by your agreement who graduated during this period and intend to work for the Department of Defense 0.00
- The number of undergraduates funded by your agreement who graduated during this period and will receive scholarships or fellowships for further studies in science, mathematics, engineering or technology fields: 0.00

Names of Personnel receiving masters degrees

<u>NAME</u>
Joshua Jae-Hyuk Lee
Ulrich Niemann
Total Number:
2

Names of personnel receiving PHDs

<u>NAME</u>
Stefan Helmuth Humer
Total Number:
1

Names of other research staff

<u>NAME</u>	<u>PERCENT SUPPORTED</u>	
Ulrich Niemann	0.21	No
Reinhard Seiser	0.50	No
Stefan Humer	1.00	No
Jae-Hyuk Lee	1.00	No
Bruce Thomas	0.11	No
FTE Equivalent:	2.82	
Total Number:	5	

Sub Contractors (DD882)

Inventions (DD882)

Autoignition and Combustion of Diesel and JP-8, Proposal Number:45241EG, Agreement Number: W911NF0410139

Contents

1	Statement of Problem Studied	2
2	Summary of the Most Important Results	2
2.1	Chemical Inhibition of Nonpremixed Methane Flames by CF_3Br	3
2.2	Rate-Ratio Asymptotic Analysis of Autoignition of <i>n</i> -Heptane in Laminar Nonpremixed Flow	4
2.3	Experimental and Kinetic Modeling Study of Combustion of JP-8, its Surrogates and Reference Components in Laminar Nonpremixed Flows	4
2.4	Experimental Investigation of Methanol and Ethanol Flames in Nonuniform Flows	5
2.5	Rate-Ratio Asymptotic Analysis of the Structure and Extinction of Partially Premixed Flames	6
2.6	Activation-Energy Asymptotic Theory of Autoignition of Condensed Hydrocarbon Fuels in Nonpremixed Flows with Comparison to Experiment	7
2.7	The Structure of Nonpremixed Toluene Flames	7
2.8	Combustion of Jet Fuels and its Surrogates in Laminar Nonuniform Flows	8
2.9	Autoignition and Extinction of Methyl-Esters in Non-Premixed Flows	8

1 Statement of Problem Studied

The Department of Defense directive # 4140.25 dated April 12, 2004 mandates that “primary fuel support for land-based air and ground forces in all theaters (overseas and in the Continental United States) shall be accomplished using a single kerosene-based fuel, in order of precedence: JP-8, commercial jet fuel (with additive package), or commercial jet fuel (without additives).” A key challenge is to develop technologies for converting diesel-powered equipment employed by the US Army so that they can be powered by JP-8. This conversion is a complicated process. Many issues with fuel properties and performance have to be considered. They include autoignition, combustion, fuel injection, lubricity, and spray characteristics.

The objective of the study described in this report is to understand those key aspects of combustion of JP-8 that are required to facilitate conversion of diesel-powered equipment to JP-8. JP-8 is a mixture of numerous aliphatic and aromatic compounds. The major components of this fuel are straight chain paraffins, branched chain paraffins, cycloparaffins, aromatics, and alkenes. The concentration of paraffins is on the average 60 % by volume, that of cycloparaffins 20 %, that of aromatics 18 %, and that of alkenes 2 %. It has been established that a useful approach is to first develop surrogates that reproduce selected aspects of combustion of JP-8. Surrogates are mixtures of hydrocarbon compounds. The hydrocarbon compounds used to construct the surrogate will depend on those aspects of combustion of JP-8 that the surrogate is expected to reproduce.

Combustion processes in diesel engines closely resemble nonpremixed systems. Therefore, the research was focused on nonpremixed flames. Experimental and numerical studies were carried out. The counterflow configuration was employed. The studies were carried out using many hydrocarbon fuels, jet fuels, and potential surrogates. Critical conditions of autoignition and critical conditions of flame extinction were measured. To characterize the structure of the reactive flow field, temperature profiles, and concentration profiles of stable species were measured. Numerical calculations were performed using detailed chemistry. The next section describes the important results obtained in this research.

2 Summary of the Most Important Results

The summaries of the important results are given in this section. Section 2.1 describes research with application to fire safety. Section 2.2 describes a simple procedure to calculate critical conditions of autoignition on *n*-heptane. This can be extended to other hydrocarbon fuels and to surrogates. Section 2.3 describes experimental and numerical studies carried out on single component fuels, jet fuels and surrogates. Section 2.4 describes experimental studies on methanol and ethanol flames. These fuels are considered as alternative fuels. Section 2.5

describes aspects of combustion in partially premixed flows. The information is of importance in modelling combustion processes taking place in practical devices. Section 2.6 describes experimental and analytical studies on components of surrogates of JP-8. Section 2.7 describes experimental studies on toluene. This is a component of surrogates of JP-8. Section 2.8 describes experimental studies on JP-8 and surrogates of JP-8. Two potential surrogates of JP-8 are suggested. Section 2.9 describes studies on surrogates of biodiesel.

The research described in sections 2.1, 2.2, 2.3, 2.4, and 2.5 have been published in peer-reviewed journals. Reprints have been sent to the Army Research Office. The research described in section 2.6 has been submitted for publication in a peer-reviewed journal. A copy of the manuscript has been sent to the Army Research Office. Manuscripts describing research described in sections 2.7, 2.8, and 2.9 are in preparations for submission to peer-reviewed journals. A draft of these manuscripts is attached to this report.

2.1 Chemical Inhibition of Nonpremixed Methane Flames by CF_3Br

Experimental, numerical, and analytical studies are carried out to elucidate the mechanisms of inhibition of nonpremixed methane flames by bromotrifluoromethane (CF_3Br). Experiments are performed in the counterflow configuration. In this configuration the reactants are injected into a mixing layer from two ducts. A fuel stream made up of methane and nitrogen (N_2) is injected from one duct, and an oxidizer stream of oxygen and N_2 is injected from the other duct. The inhibitor CF_3Br is either added to the oxidizer stream or to the fuel stream. A key objective of this study is to compare chemical inhibition of methane flames when CF_3Br is added to the oxidizer stream with that when this inhibitor is added to the fuel stream. Critical conditions of extinction are measured. The concentrations of reactants at the boundaries are so chosen that the values of stoichiometric mixture, ξ_{st} , and adiabatic temperature, T_{st} , are the same. Numerical calculations are performed using a detailed chemical-kinetic mechanism. A reduced chemical-kinetic mechanism made up of eight global steps is derived from this detailed mechanism. Rate-ratio asymptotic analysis is carried out using this reduced mechanism. Experimental data, numerical calculations, and results of asymptotic analysis show that CF_3Br is more effective in inhibiting methane flames when it is added to the oxidizer stream when compared with its effectiveness when it is added to the fuel stream. The elementary reaction $\text{H} + \text{Br}_2 \rightarrow \text{HBr} + \text{Br}$ plays a central role in the inhibition when CF_3Br is added to the oxidizer stream. This reaction, however, has negligible influence on critical conditions of extinction when CF_3Br is added to the fuel stream.

2.2 Rate-Ratio Asymptotic Analysis of Autoignition of *n*-Heptane in Laminar Nonpremixed Flow

The research described here was carried out in collaboration with Professor N. Peters, N., and Mr. G. Paczko, at RWTH Aachen, Germany.

A rate ratio asymptotic analysis is carried out to elucidate the mechanisms of autoignition of *n*-heptane (C_7H_{16}) in laminar, nonpremixed flows. It has been previously established that autoignition of *n*-heptane takes place in three distinct regimes. These regimes are called the low-temperature regime, the intermediate temperature regime and the high temperature regime. The present analysis considers the high temperature regime. A reduced chemical-kinetic mechanism made up of two global steps is used in the analysis. The reduced mechanism is deduced from a skeletal mechanism made up of 16 elementary reactions. The skeletal mechanism is derived from a short mechanism made up of 30 elementary reactions. The short mechanism is deduced from a detailed mechanism made up of 56 elementary reactions. In the reduced mechanism, the first global step represents a sequence of fast reactions starting from the rate limiting elementary reaction between *n*-heptane and HO_2 . In this global step C_7H_{16} is consumed and hydrogen peroxide (H_2O_2) is formed. The second global step represents a sequence of fast reactions starting from the rate limiting elementary reaction in which H_2O_2 is consumed and OH is formed. A key aspect of the second global step is that the sequence of fast reactions gives rise to consumption of fuel only without net consumption of H_2O_2 . This makes the chemical system auto-catalytic. The unsteady flamelet equations are used to predict the onset of autoignition. In the flamelet equations a conserved scalar quantity, Z , is used as the independent variable. On the oxidizer side of the mixing layer $Z = 0$, and on the fuel side $Z = 1$. The practical case where the temperature of the oxidizer stream, T_2 , is much greater than the temperature of the fuel stream is considered. Therefore autoignition is presumed to take place close to $Z = 0$. Balance equations are written for C_7H_{16} and H_2O_2 . It is postulated that autoignition will take place when the gradient of mass fraction fuel with respect Z , evaluated at $Z = 0$, is zero. The value of T_2 when autoignition takes place is obtained as a function of the strain rate. These critical conditions of autoignition obtained from asymptotic analysis agree well with those calculated using the detailed mechanism and the skeletal mechanism.

2.3 Experimental and Kinetic Modeling Study of Combustion of JP-8, its Surrogates and Reference Components in Laminar Nonpremixed Flows

The research described in this section was carried out in collaboration with Professor Mr. A. Frassoldati, Ms. S. Granata, Mr. T. Faravelli, and Professor E. Ranzi, at Dipartimento di Chimica, Materiali e Ingegneria Chimica, Politecnico di Milano, 20133 Milano, Italy.

Experimental and numerical studies are carried out to construct reliable surrogates that can reproduce aspects of combustion of JP-8 and Jet-A. Surrogate fuels are defined as mixtures of few hydrocarbon compounds with combustion characteristics similar to those of commercial fuels. The combustion characteristics considered here are extinction and autoignition in laminar nonpremixed flows. The “reference” fuels used as components for the surrogates of jet fuels are *n*-decane, *n*-dodecane, methylcyclohexane, toluene, and *o*-xylene. Three surrogates are constructed by mixing these components in proportions to their chemical types found in jet fuels. Experiments are conducted in the counterflow system. The fuels tested are the components of the surrogates, the surrogates, and the jet fuels. A fuel stream made up of a mixture of fuel vapors and nitrogen is injected into a mixing layer from one duct of a counterflow burner. Air is injected from the other duct into the same mixing layer. The strain rate at extinction is measured as a function of the mass fraction of fuel in the fuel stream. The temperature of the air at autoignition is measured as a function of the strain rate at a fixed value of the mass fraction of fuel in the fuel stream. The measured values of the critical conditions of extinction and autoignition for the surrogates show that they are slightly more reactive than the jet fuels. Numerical calculations are carried out using a semi-detailed chemical-kinetic mechanism. The calculated values of the critical conditions of extinction and autoignition for the reference fuels and for the surrogates are found to agree well with experimental data. Sensitivity analysis is used to highlight key elementary reactions that influence the critical conditions of autoignition of an alkane fuel and an aromatic fuel.

2.4 Experimental Investigation of Methanol and Ethanol Flames in Nonuniform Flows

Experimental studies are conducted on extinction and autoignition of methanol and ethanol flames in laminar, nonuniform flows. Two flame types are considered: nonpremixed and premixed. The studies are performed in the counterflow configuration. The burner used in the experiments is made up of two ducts. Studies in the nonpremixed configuration are carried out by injecting a stream comprised of fuel vapors and nitrogen from one duct, and a stream of air from the other duct. In the premixed configuration a premixed-reactant stream made up of fuel vapors, air, and nitrogen, is injected from one duct, and a nitrogen stream from the other duct. Numerical calculations are performed using detailed chemistry at conditions corresponding to those used in the experiments. For the nonpremixed systems considered here, the calculated values of the critical conditions of extinction agree well with experimental data. At given values of the strain rate and temperature of the fuel stream, the calculated temperature of the oxidizer stream at autoignition is found to be higher than the measured values. In the premixed configuration the strain rate at extinction is measured for various values of the equivalence ratio of the mixture in the premixed-reactant stream, ϕ_1 . The value of ϕ_1 , at

which the calculated extinction strain rate is the highest, is found to be larger than the value of ϕ_1 at which the measured extinction strain rate is the highest. Sensitivity analysis is carried out to test the influence of various elementary reactions on critical conditions of extinction. The structure of a nonpremixed methanol flame is investigated. Concentration profiles of stable species and temperature profiles are measured. The flame structure is calculated using detailed chemistry. The results of numerical calculations agree well with experimental data.

2.5 Rate-Ratio Asymptotic Analysis of the Structure and Extinction of Partially Premixed Flames

The research described in this section was carried on in collaboration with Professor X. S. Bai at Lund University of Technology, Lund, Sweden.

Rate-ratio asymptotic analysis is carried out to elucidate the structure and mechanisms of extinction of laminar, partially premixed methane flames. A reduced chemical-kinetic mechanism made up of four global steps is used. The counterflow configuration is employed. This configuration considers a flame established between a stream of premixed fuel-rich mixture of methane (CH_4), oxygen (O_2), and nitrogen (N_2) and a stream of fuel-lean mixture of CH_4 , O_2 , and N_2 . The objective of the study is to characterize the influence of premixing one reactant stream of a nonpremixed system with the other reactant on structures and critical conditions of extinction. The levels of premixing are given by the equivalence ratios ϕ_r of the fuel-rich mixture and ϕ_l of the fuel-lean mixture. The mass fraction of the reactants at the boundaries are so chosen that the diffusive flux of reactants entering the reaction zone is the same for all values of ϕ_r and ϕ_l considered in the analysis. The analysis shows that the value of the scalar dissipation rate at extinction increases with increasing ϕ_l for $\phi_r^{-1} = 0$ while it decreases with increasing ϕ_r^{-1} for $\phi_l = 0$. The results of the analysis agree with numerical calculations carried out using a chemical-kinetic mechanism made up of elementary reactions. They also agree with experimental data. A key finding is that at fixed values of the scalar dissipation rate, the leakage of oxygen from the reaction zone to the inert regions outside the reaction zone decreases with increasing ϕ_l . As a consequence the flame temperature increases. This makes the flame more resistant to strain. At fixed values of the scalar dissipation rate, the leakage of oxygen from the reaction zone increases with increasing values of ϕ_r^{-1} . This makes the flame less resistant to strain.

2.6 Activation-Energy Asymptotic Theory of Autoignition of Condensed Hydrocarbon Fuels in Nonpremixed Flows with Comparison to Experiment

An activation-energy asymptotic theory is developed that predicts autoignition of condensed hydrocarbon fuels in nonpremixed flows. Steady, laminar, stagnation-point flow of an oxidizer stream, toward the vaporizing surface of a liquid fuel is considered. The analysis is restricted to the case where the temperature of the oxidizer stream, T_2 , is greater than the normal boiling point of the liquid fuel. The gas-phase chemical reaction is described by a one-step overall process. The chemical-kinetic rate parameters are the activation temperature, T_a , and the frequency factor, B . A Zel'dovich number, β , is constructed that is proportional to the ratio T_a/T_2 . The analysis is performed in the asymptotic limit of large values of β . It predicts the value of the Damköhler number, at autoignition. The Damköhler number is defined as the ratio a characteristic flow time to a characteristic chemical reaction time. The flow time is the reciprocal of the strain rate, and the chemical time depends on the chemical-kinetic rate parameters. To illustrate the application of the results of the analysis, experiments are conducted in the counterflow configuration. Fuels tested are *n*-heptane, *n*-octane, *n*-decane, *n*-dodecane, *n*-hexadecane, *iso*-octane, cyclohexane, methylcyclohexane, *o*-xylene, JP-10, JP-8, and diesel. The temperature of the oxidizer stream at autoignition is measured for various values of the strain rate. The strain rate, and the value of the Damköhler number at autoignition, obtained from the analysis, are used to obtain the chemical-kinetic rate parameters, for the fuels tested here. Critical conditions of extinction of flames burning these liquid fuels are also measured. A key finding of this work is that for the straight-chain alkanes tested here, at a given value of the strain rate, *n*-heptane is the most difficult to ignite followed by *n*-octane, *n*-decane, *n*-dodecane, and *n*-hexadecane. The order is reversed for extinction, here it is found that flames burning *n*-heptane and *n*-octane are the most difficult to extinguish followed by *n*-decane, *n*-dodecane, and *n*-hexadecane.

2.7 The Structure of Nonpremixed Toluene Flames

Experimental and numerical studies are performed to elucidate the structure and mechanisms of extinction and autoignition of toluene flames in a counterflow configuration under nonpremixed conditions. Experiments are conducted in a flame stabilized between two opposing streams. The fuel stream is a mixture of prevaporized toluene and nitrogen, and the oxidizer stream consists of ambient air. Concentration profiles of C_7H_8 (toluene), O_2 , N_2 , CO_2 , CO , H_2O , CH_4 , and C_2H_6 (benzene), and hydrocarbons ranging from C_2 up to C_5 are measured. The profiles of stable species are measured over the distance between the two opposing ducts by taking gas samples from the flame using a small quartz microprobe. The gas samples are analyzed using a gas chromatograph. Temperature profiles are measured using a thermocou-

ple. Critical conditions of extinction are measured. Critical condition of autoignition are also obtained evaluating the fuel mole fraction and the temperature of the oxidizer stream as a function of the strain rate. Numerical calculations are performed using detailed chemistry to determine the flame structure. These results are compared with the the measurements.

2.8 Combustion of Jet Fuels and its Surrogates in Laminar Nonuniform Flows

Experimental studies are carried out to characterize nonpremixed combustion of jet fuels and a number of its surrogates in laminar nonuniform flows. The counterflow configuration is employed. Critical conditions of extinction and autoignition are measured for JP-8, Jet-A, and Fisher Tropsch (FT) JP-8. Fifteen surrogates of JP-8 and one surrogate of FT JP-8 are tested. It is found that critical conditions of extinction and autoignition of JP-8 and Jet-A are similar, while FT JP-8 is more reactive than JP-8 and Jet-A. Among the surrogates tested, the Aachen surrogate made up of *n*-decane (80 %) and trimethylbenzene (20 %) by liquid volume, and the UCSD surrogate made up of *n*-dodecane (60 %), methylcyclohexane (20 %), and *o*-xylene (20 %) by liquid volume best reproduce extinction and autoignition characteristics of JP-8. Surrogate G made up of *n*-decane (60 %) and iso-octane (40 %) by liquid volume best reproduces the combustion characteristics of FT JP-8.

2.9 Autoignition and Extinction of Methyl-Esters in Non-Premixed Flows

Biodiesel is defined as mono-alkyl esters of long chain fatty acids derived from vegetable oils. It contains no petroleum, but it can be blended at any level with petroleum diesel to create a biodiesel blend. An improved understanding of the combustion characteristics of esters can provide insights on combustion of biodiesel. Critical conditions of extinction and autoignition are measured for diesel, biodiesel and a number of esters in nonuniform flow fields under non-premixed conditions. The esters considered are methyl butanoate, methyl crotonate, and ethyl propionate. Methyl butanoate is considered to be a surrogate for biodiesel. The counterflow configuration is employed. The strain rate at extinction is measured as a function of the composition of the reactant streams of the counterflow system. In the autoignition experiments, the temperature of air is increased until autoignition is obtained. The temperature of air at autoignition is measured for various values of strain rate. Numerical calculations are performed using a previously developed chemical-kinetic mechanism for methyl butanoate. The critical conditions of extinction and autoignition calculated using this mechanism is found to agree well with experimental data.

The Structure of Nonpremixed Toluene Flames

J. J. Lee^{1,2}, S. Humer^{1,2}, R. Seiser¹, K. Seshadri*¹, E. Pucher²

¹Department of Mechanical and Aerospace Engineering
University of California, San Diego
La Jolla, California 92093-0411, USA

²Institute for Internal Combustion Engines and Automotive Engineering
Vienna University of Technology
A-1040 Vienna, Austria

Abstract

Experimental and numerical studies were performed to elucidate the structure and mechanisms of extinction of toluene flames in a counterflow configuration under nonpremixed conditions. Experiments are conducted on flames stabilized between two opposing streams. The fuel stream is a mixture of prevaporized toluene and nitrogen, and the oxidizer stream consists of ambient air. Concentration profiles of C_7H_8 (toluene), O_2 , N_2 , CO_2 , CO , H_2O , CH_4 , C_6H_6 (benzene), and hydrocarbons ranging from C_2 up to C_5 are measured. The profiles of species are measured over the distance between the two opposing ducts by taking gas samples from the flame using a small quartz microprobe. The gas samples are analyzed in a gas chromatograph. Temperature profiles are measured using a thermocouple. Critical conditions of extinction are measured. Critical conditions of autoignition are also obtained evaluating the fuel mole fraction and the temperature of the oxidizer stream as a function of the strain rate. Numerical calculations are performed using detailed chemistry to determine the flame structure. These results are compared with the measurements.

Introduction

Gaseous fuels have seen a higher interest of research in comparison to liquid fuels. This happened because of the much higher complexity of liquid fuels in handling and operation of experiments but also because the mechanisms of smaller hydrocarbons are the basis for investigating the mechanisms of larger ones. The research on toluene is of interest since it is a typical representative of the thousands of components of gasoline, diesel, and aviation jet fuel. Toluene (C_7H_8) is a member of the aromatic-fuel group. It is a natural component of crude oil, out of which gasoline, diesel fuel, aviation fuel, and other fuels are produced. Toluene itself is produced by distillation from gasoline streams and is used as a high octane blending component. Diesel and aviation fuel consist of approximately 29 vol% [1, 2], and 18 vol% [3] aromatics, respectively. Furthermore, it has been proposed to use toluene as a surrogate for describing aromatics in combustion of diesel and aviation jet fuel.

Therefore detailed data of oxidation chemistry of aromatics are important to accurately model the combustion process of the above mentioned fuels.

The combustion of toluene has been studied experimentally by various investigators. Previous studies were conducted on shock tubes [4-6], jet-stirred reactors [4], flow reactors [5-10], and rapid compression machines [11, 12]. Most of these experiments were conducted on premixed systems. In this work experimental data obtained from a non-premixed toluene flame in a counterflow configuration are presented. In the following the experimental setup and method are described, and data for stable species and temperatures are reported. Additionally, data for extinction and autoignition are provided. Numerical calculations are conducted and compared with the experimental data.

Experimental and Numerical Studies

In this study a nonpremixed toluene flame is stabilized in a counterflow configuration. Figure 1

*Corresponding author: seshadri@mae.ucsd.edu

shows a schematic illustration of the counterflow configuration with the setup for temperature and species concentration measurements. Two ducts, each one surrounded by an outer concentric duct are opposing each other. A diluted fuel-nitrogen mixture, containing prevaporized toluene with a mole fraction of $X_{C_7H_8} = 0.15$ and nitrogen, exits from the lower inner duct (referred to as fuel duct), ambient air exits from the upper inner one (referred to as oxidizer duct). Both outer ducts (referred to as curtain ducts) carry nitrogen flows. The flows are regarded to be laminar, steady, and axisymmetric. The curtain flows prevent any influence from the surrounding air. In the mixing region between the ducts a stagnation plane is formed. The experiments are conducted at a strain rate $a_2 = 100s^{-1}$, which is calculated by following formula [13].

$$a_2 = \frac{2|V_2|}{L} \left(1 + \frac{|V_1|\sqrt{\rho_1}}{|V_2|\sqrt{\rho_2}} \right) \quad (1)$$

Here ρ denotes the density and V the velocity at the duct exit. Subscripts 1 and 2 refer to the fuel stream and oxidizer stream, respectively. The separation distance between the opposing ducts is given by $L=10$ mm. The momentums between the two opposing streams are balanced as described by $\rho_1 V_1^2 = \rho_2 V_2^2$. Plug flow boundary conditions are assumed. Details and dimensions of the counterflow burner are given in Refs. [14-16].

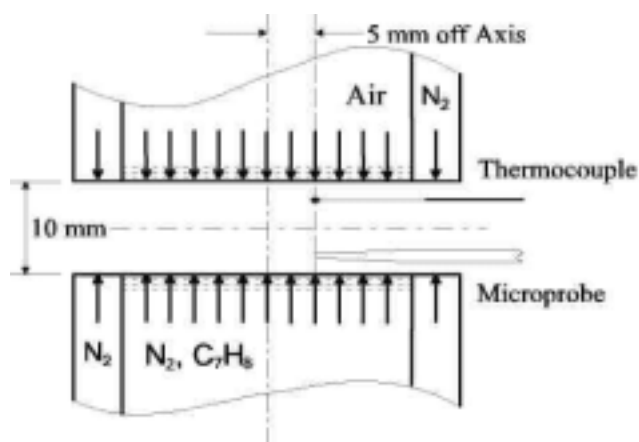


Figure 1. Schematic illustration of the counterflow configuration employed for temperature and species measurement in a nonpremixed toluene flame. An uncoated Pt-Pt 13% Rh (type R) thermocouple is used for the temperature measurements. Gas samples are removed using a quartz microprobe.

To measure the concentration of stable species, gas samples are removed from the reaction zone using two types of quartz microprobes. The gas samples are analyzed in a gas chromatograph. The tips of the handmade microprobes have outer diameters of 225 microns and 180 microns, and inner diameters of 126 microns and 117 microns, respectively. A tapered copper shield is attached around the tip of the probe to reduce heat transfer from the flame to the front thin part of the probe in order to prevent and to minimize further reactions of the gas after sampling. The probe, all sampling lines, and the sample loop of the gas chromatograph are held at approximately 350 K. By proper balance of this temperature with the pressure of the sampling lines and the sample loop, condensation of sampled vapor is prevented. The inside of the probe was filled with glass-fiber to filter out the soot and to prevent that it reaches the gas chromatograph. For the temperature measurement a thermocouple is employed. As shown in Fig. 1, the location of the tip of the probe is placed 5 mm off the center line to avoid any disturbance of the flow field and any influence on the reactive diffusive balance in the vicinity of the probe. It is assumed that the species concentrations and temperatures are only functions of the vertical coordinate [17]. The gas samples are analyzed in a SRI 8610C gas chromatograph. The instrument is equipped with a 4.5ft mole-sieve (80/100 mesh) - for separation of H_2 , O_2 , Ar, N_2 , CH_4 , and CO - and a 12ft long Poropak Q column for separating all other species. To optimize the performance of both columns, temperature programming and valve switching is employed. After the species are separated in the columns they are quantified by a thermo-conductivity-detector (TCD) and a flame-ionization-detector (FID). The chromatograms are analyzed by in-house software comparing measurements of known gas-samples to determine the absolute mole fraction. For species that were not previously calibrated, calibration factors are determined by inter- and extra-polation around known species. This was done by plotting the FID-calibration factors as a function of the number of C-atoms. In one curve for paraffins, species measured consist of ethane and propane. A second curve for the alkenes was similarly established by calibrating ethene, propene, 1-butene, 1-pentene, and 1-hexene. All species of C_4 -hydrocarbons are reported as one concentration because separation into single components and calibration was not possible. Similarly C_5 and C_6 -hydrocarbons are reported, assuming that they are mostly made up of 1-alkenes, using the 1-alkene calibration. Only benzene (C_6H_6) can be separated

from other C_6 -species, and therefore the concentration of this could be determined. Ethene and ethyne appear in the gas chromatogram as a single peak and are reported as their sum using the calibration for ethene. Argon eludes together with oxygen from the columns of the gas chromatograph. By assuming the Lewis number of argon and the Lewis number of the main species to be equal, the amount of argon at any point in the flow-field is determined from the mixture fraction (calculated using the carbon mass fraction from the measured species) and the amount of argon in the oxidizer stream ($Y_{Ar} = 0.01313$) [18]. The error for the maximum concentration of O_2 , N_2 , CO_2 , and CO is expected to be less than $\pm 10\%$. These species can be clearly identified by the TCD-detector. The error for the maximum concentration of CH_4 , $C_2H_2+C_2H_4$, C_2H_6 , C_3H_6 , C_3H_8 , C_4^- , C_5^- , C_6H_6 , and C_7H_8 species is expected to be less than $\pm 5\%$. These species can be clearly identified by the FID-detector and the disturbance of the signal due to noise is very low. Hydrogen gives a very small signal on the TCD-detector, and therefore its accuracy is expected to be only better than $\pm 30\%$. The signal for water appeared as peak with a long tail on the TCD-detector. The area of this peak was determined by using a linear baseline starting at the onset of the water signal and parallel to the baseline for a measurement containing no water. An accuracy of better than $\pm 20\%$ is expected for water. The temperature profile was established by using an uncoated Pt-Pt13%Rh (type R) thermocouple with a wire diameter of 25 microns and a bead diameter of 182 microns. Radiation of the thermocouple was taken into account, assuming a spherical shape of the bead and a constant emissivity of 0.2 [19]. Catalytic effects are neglected. The error of the temperature measurements is better than ± 60 K. The influence of soot on the temperature measurements is presumed to be small. A digital camera and an image processing software with a coordinate evaluation feature was utilized to determine the location of the sampling probe and the thermocouple in the flow field. The accuracy of the position determination is approximately 50 microns.

The extinction experiments result in a plot of the fuel mole fraction over the strain rate at extinction. Therefore a flame with a certain fuel/nitrogen mixture is stabilized between the ducts, and the strain rate is increased step by step until the flame extinguishes. Autoignition results show the ignition temperature as a function of the strain rate. At a fixed fuel mole-fraction of $X_{C_7H_8} = 0.15$, the oxidizer stream is heated up

slowly until autoignition occurs. The separation distance between the two ducts for the extinction and the autoignition experiments are $L=10$ mm and $L=12$ mm, respectively. The temperature of the fuel stream is 375 K for both experiments and the oxidizer stream 299 K for the extinction experiments.

The same boundary conditions as in the experiments are applied to perform the numerical calculations using detailed chemistry. It is assumed that the experimental setup satisfies plug-flow boundary conditions, and buoyancy is neglected. The computer program FlameMaster which was developed at RWTH-Aachen is used for the numerical calculations [20]. The conservation equations of mass, momentum, and energy and species balance equations used in the formulation of the numerical problem are summarized elsewhere [20-22]. The species balance equations include thermal diffusion, and the energy conservation equation includes radiative heat losses from carbon dioxide and water vapor [20]. A detailed chemical kinetic mechanism for toluene containing 379 species was assembled by Pitz et al. [23]. Solutions could not be obtained with the 379 species detailed mechanism due to numerical "stiffness" problems. Therefore it was reduced to a detailed chemical kinetic mechanism containing 58 species with 215 reversible reactions [24] which is used for the numerical calculations.

Results and Discussion

Figure 2 shows experimental data on the temperature field in the nonpremixed toluene flame. The temperature of the thermocouple is plotted by the triangles. Taking into account the radiation from the surface of the thermocouple, the actual gas temperature is evaluated and plotted using circles in Fig. 2. The maximum temperature of the corrected temperature profile is 1739 K and slightly higher than the maximum temperature of the computation which is 1680 K, and the peak of the measurements is closer to the fuel side. The temperature profile of the measurements is broader than the results from the numerical calculation. Furthermore, the data of the numerical computation appear shifted to the oxidizer side by approximately 300 microns compared to the results of the experimental measurements, not solely for the temperature profile but also for all concentration profiles. The profile of the main species in the toluene flame can be seen in Fig. 3. The profile of the measured and the calculated concentrations agree very well besides the shift. The main products of combustion of hydrocarbons - CO_2 , H_2O , and CO - are

usually well predicted by chemical-kinetic mechanisms. The CO profile is broader and the O₂ leakage is higher than expected by the calculation. Figure 4 shows experimental data on intermediate species of small molecular weight. The maximum concentration of C₂H₂+C₂H₄ is overpredicted by about 80% whereas for CH₄ the calculation corresponds pretty well. Figure 5 shows the profiles of H₂ and benzene. The numerical computations overpredict the presence of benzene in the toluene flame by about 30%, whereas hydrogen is underpredicted in the computations by almost the factor 2. Figure 6 shows experimental data on concentrations of stable hydrocarbon species like C₃H₆ and larger. These species but also C₂H₆ in Fig. 4 are not represented in the chemical-kinetic mechanism and therefore no corresponding computational data are plotted. Figure 7 shows experimental data on extinction of a nonpremixed toluene flame with variable fuel concentrations. Figure 8 shows experimental data on autoignition of a nonpremixed toluene / air system.

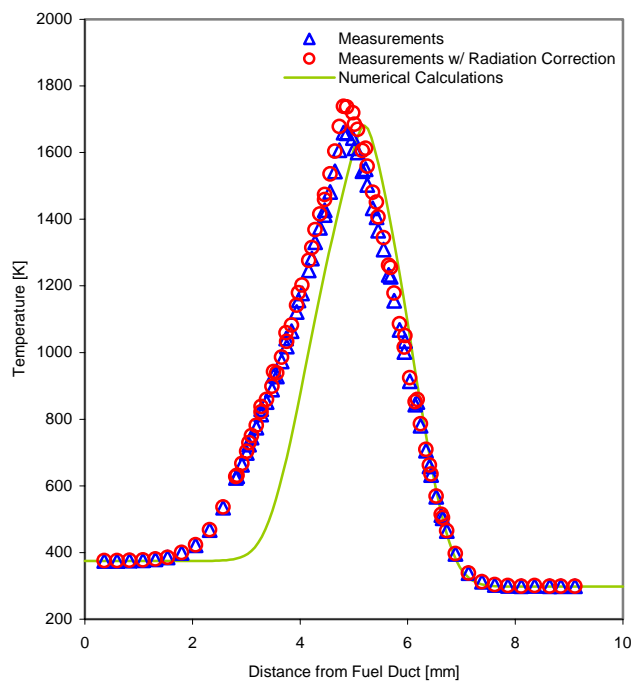


Figure 2. Temperature Measurement in a nonpremixed toluene flame. The triangles represent the measured temperature using a thermocouple, the circles represent the measured temperature corrected for radiation losses. The line is the result of the numerical calculation using detailed chemistry.

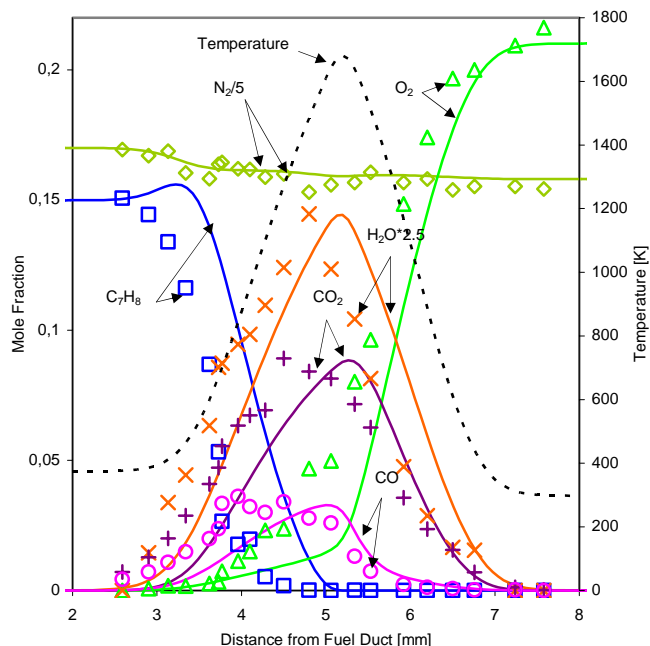


Figure 3. Experimental data showing the mole fraction of toluene, O₂, N₂, CO, CO₂, and H₂O as a function of distance. The points represent the experimental data, and the lines are results of the numerical calculations. The numerically computed temperature is shown for reference.

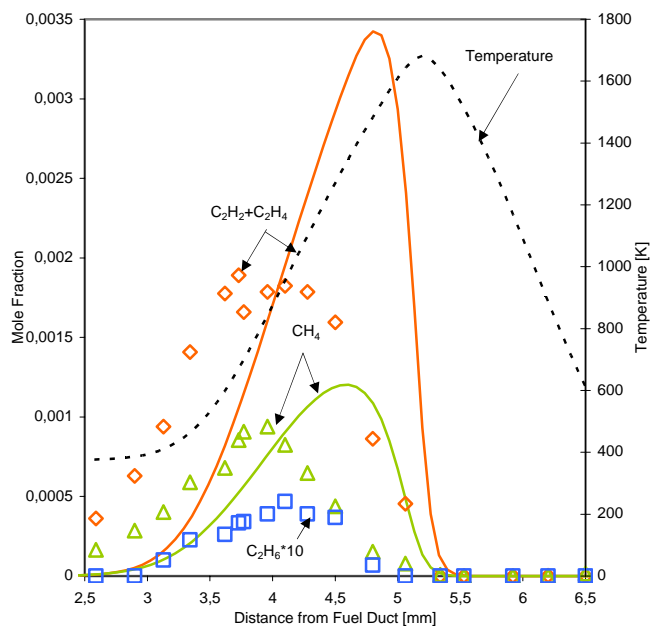


Figure 4. Experimental data showing the mole fraction of C₂H₂+C₂H₄, CH₄, and C₂H₆ as a function of distance. The points represent the experimental data, and the lines are results of numerical calculations. The numerically computed temperature is shown for reference.

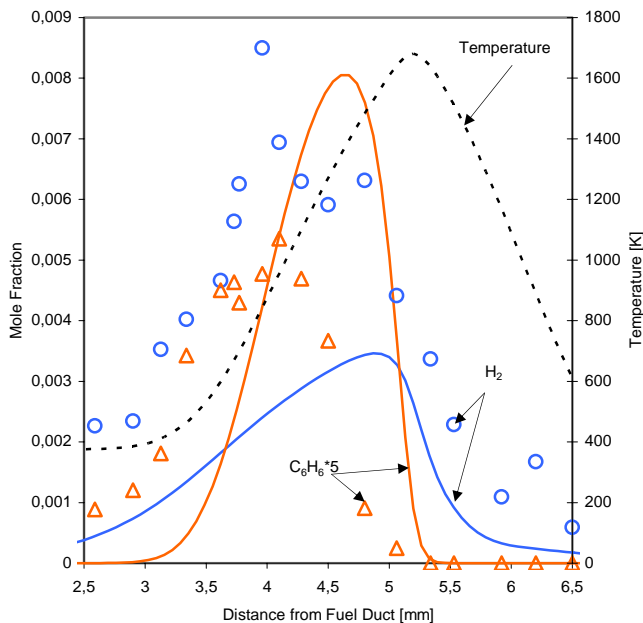


Figure 5. Experimental data showing the mole fraction of H_2 and C_6H_6 as a function of distance. The points represent the experimental data, and the lines are results of numerical calculations. The numerically computed temperature is shown for reference.

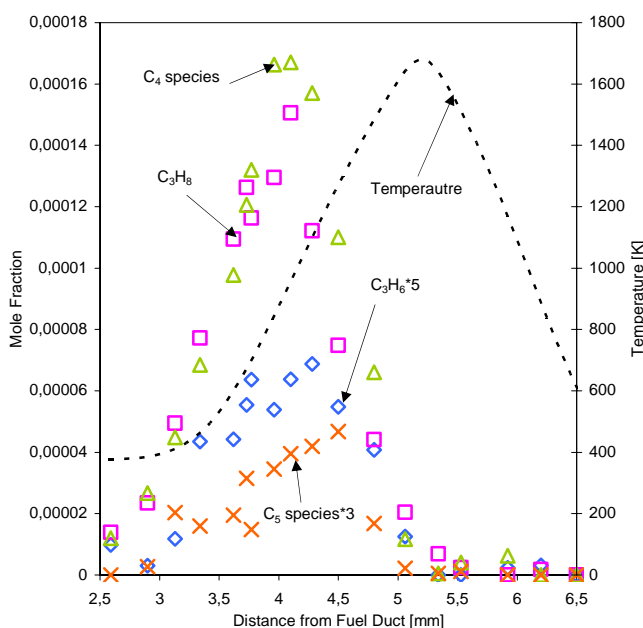


Figure 6. Experimental data showing the mole fraction of C_3H_6 , C_3H_8 , C_4^- , and C_5 -hydrocarbons as a function of distance. The points represent the experimental data. The numerically computed temperature is shown for reference.

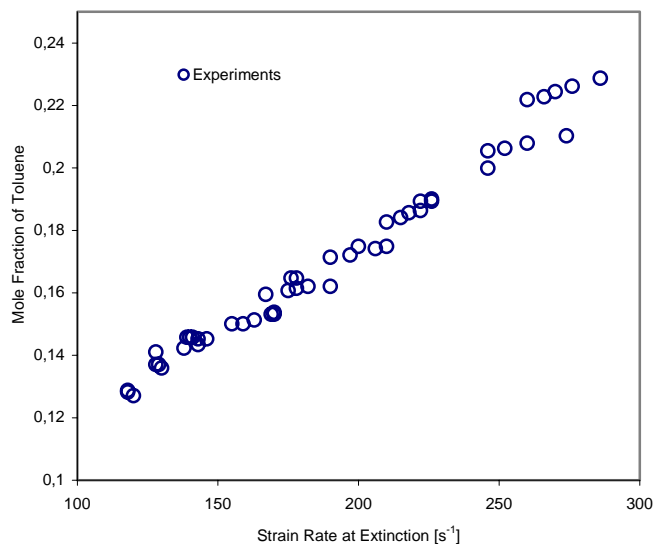


Figure 7. Extinction of nonpremixed toluene flames. The mole fraction of toluene in the fuel stream is plotted over the strain rate. The oxidizer stream is air. The temperatures of the fuel stream and oxidizer stream are 375 K and 299 K, respectively, and the measurements are shown by the circles.

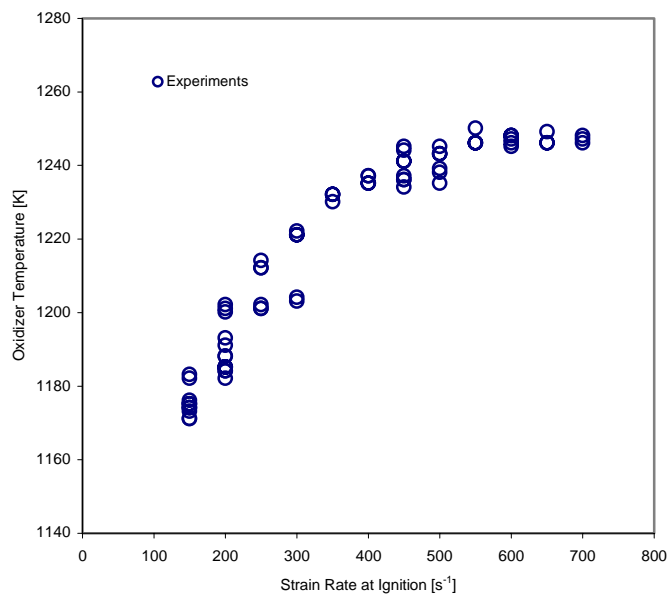


Figure 8. Autoignition of nonpremixed toluene flames. The oxidizer temperature at autoignition is plotted over the strain rate. The mole fraction of toluene in the fuel stream is 0.15. The oxidizer stream is air. The measurements are shown by the circles.

Acknowledgments

The research is supported by the US Army Research Office.

REFERENCES

1. Wenck H. und Schneider C., *DGMK-Projekt 409: Chemisch-physikalische Daten von Otto- und Dieselmotoren*. Technical report, DGMK Deutsche wissenschaftliche Gesellschaft für Erdöl, Erdgas und Kohle e. V., Hamburg, November 1993.
2. Flynn P., *Concentration of various hydrocarbon compounds in diesel*. Cummins, private communication, 1998.
3. Edwards T. and Maurice L. Q., *Surrogate mixtures to represent complex aviation and rocket fuels*. *Journal of Propulsion and Power*, 17:461-466 (2001).
4. Dagaut P., Pengloan G., and Ristori A., *Phys. Chem. Chem. Phys.* 4:1846-1854 (2002).
5. Hamins A., *The structure and extinction of diffusion flames*, Ph.D. thesis, University of California at San Diego, 1985.
6. Hamins A. and Seshadri K., *Combustion and Flame* 68:295-307 (1987).
7. Klotz S.D., Brezinsky K., and Glassmann I., *Proceedings of the Combustion Institute* 27:337-344 (1998).
8. Emdee J.L., Brezinsky K., and Glassmann I., *Journal of Physical Chemistry* 96:2151-2161 (1992).
9. Venkat C., Brezinsky K., and Glassmann I., *Proceedings of the Combustion Institute* 19:143-152 (1982).
10. Brezinsky K., Litzinger T.A., and Glassmann I., *International Journal of Chemical Kinetics* 16:1053 (1984).
11. Griffiths J.F., Halford-Maw P.A., and Rose D.J., *Combustion and Flame* 95:291-306 (1993).
12. Roubaud A., Minetti R., and Sochet L.R., *Combustion and Flame* 121:535-541 (2000).
13. Seshadri K. and Williams F.A., *International Journal of Heat and Mass Transfer* 21, 2:251-253 (1978).
14. Lee J.J., *Autoignition of Diesel Fuels - The Structure of Nonpremixed Toluene Flames*, Diploma thesis, Vienna University of Technology, Austria, 2004.
15. Seiser R., *Nonpremixed combustion of liquid hydrocarbon fuels*, Ph.D. thesis, Technical University of Graz, Austria, 2000.
16. Humer S., Seiser R., and Seshadri K., *Proceedings of the Combustion Institute* 29:1597-1604 (2002).
17. Fendell F.E., *Journal of Fluid Mechanics* 21, 2:281-303 (1965).
18. Tanoue K., Seiser R., and Seshadri K., *The Structure of Nonpremixed n-decane Flames*, Paper #A31. Third Joint Meeting of the US Sections of the Combustion Institute, Chicago, Illinois (2003).
19. Thomas Weissweiler, *Measurements of stable species and soot volume fraction in a propane-air counterflow diffusion flame*, Diploma thesis, RWTH Aachen, Germany, 1994.
20. Pitsch H., *Entwicklung eines Programmpaketes zur Berechnung eindimensionaler Flammen am Beispiel einer Gegenstromdiffusionsflamme*, Master's thesis, RWTH Aachen, Germany, 1993.
21. Bollig M., Pitsch H., Hewson J.C., and Seshadri K., *Proceedings of the Combustion Institute* 26:729-737 (1996).
22. Peters N., Peters N. and Rogg B. (eds.), *Reduced Kinetic Mechanisms for Applications in Combustion Systems*, vol m15 of *Lecture Notes in Physics*, Springer-Verlag, Heidelberg, 1993, chap. 1, pp.1-13.
23. W.J. Pitz, R. Seiser, J.W. Bozzelli, I. Da Costa, R. Fournet, F. Billaud, F. Battin-Leclerc, K. Seshadri, and C.K. Westbrook, *Chemical kinetic characterization of combustion of toluene*, Paper #253. Second Joint Meeting of the US Sections of the Combustion Institute, Oakland, California (2001).
24. *Chemical-kinetic Mechanism for Toluene*, <http://combustion.ucsd.edu/mechanisms>, 2004.

5th US Combustion Meeting
Organized by the Western States Section of the Combustion Institute
and Hosted by the University of California at San Diego
March 25-28, 2007.

Combustion of Jet Fuels and its Surrogates in Laminar Nonuniform Flows

Stefan Humer⁽¹⁾ *Kalyanasundaram Seshadri*⁽¹⁾ *Reinhard Seiser*⁽²⁾

⁽¹⁾*Department of Mechanical and Aerospace Engineering,
University of California at San Diego, La Jolla, California 92093-0411, USA*

⁽²⁾*Oryxe Energy International, Inc.
Irvine, California*

Experimental studies are carried out to characterize non premixed combustion of jet fuels and a number of its surrogates in laminar nonuniform flows. The counterflow configuration is employed. Critical conditions of extinction and autoignition are measured for JP-8, Jet-A, and Fisher Tropsch (FT) JP-8. Fifteen surrogates of JP-8 and one surrogate of FT JP-8 are tested. It is found that critical conditions of extinction and autoignition of JP-8 and Jet-A are similar, while FT JP-8 is more reactive than JP-8 and Jet-A. Among the surrogates tested, the Aachen surrogate made up of *n*-decane (80 %) and trimethylbenzene (20 %) by liquid volume, and the UCSD surrogate made up of *n*-dodecane (60 %), methylcyclohexane (20 %), and *o*-xylene (20 %) by liquid volume best reproduce extinction and autoignition characteristics of JP-8. Surrogate G made up of *n*-decane (60 %) and iso-octane (40 %) by liquid volume best reproduces the combustion characteristics of FT JP-8.

1 Introduction

Developing chemical-kinetic models that describe combustion of commercial fuels is of practical importance [1, 2]. Practical fuels, for example, gasoline, diesel, and jet fuels comprise hundreds of aliphatic and aromatic hydrocarbon compounds. The focus of the present work is on jet fuels. The major components of jet fuels are straight chain paraffins, branched chain paraffins, cycloparaffins, aromatics, and alkenes [3, 4]. JP-8 is a “kerosene” fuel used by the U.S. Air Force. Detailed chemical-kinetic mechanisms describing combustion for many of the components in JP-8 are not available. A useful approach in developing chemical-kinetic mechanisms for jet fuels is to first develop surrogates for these fuels. Surrogate fuels are defined as mixtures of few hydrocarbon compounds whose relative concentrations can be adjusted so that the physical and chemical properties pertinent to combustion approximate those of commercial fuels [2].

Here, an experimental investigation is carried out with the aim of developing an appropriate surrogate for JP-8 and Fisher Tropsch (FT) JP-8. The counterflow configuration is employed. Critical conditions of extinction and autoignition are measured for various jet fuels in non premixed systems. Similar measurements are made for potential surrogates of these fuels.

2 Experimental Apparatus and Procedures

Figure 1 shows a schematic illustration of the experimental setup. The liquid fuels are vaporized using a vaporizer. A thermocouple is used to monitor the temperature inside the vaporizer. The flow rates of gases are adjusted by computer-regulated mass flow controllers. The flow lines were heated to prevent condensation. A detailed description of the burner is given elsewhere [5, 6].

In the burner a fuel stream made up of prevaporized fuel and nitrogen is injected from the fuel-duct, and an oxidizer stream of air is injected from the oxidizer-duct. These jets flow into the mixing layer between the two ducts. The exit of the fuel-duct is called the fuel boundary, and the exit of the oxidizer-duct the oxidizer boundary. The mass fraction of fuel, the temperature, and the component of the flow velocity normal to the stagnation plane at the fuel boundary are represented by $Y_{F,1}$, T_1 , and V_1 , respectively. The mass fraction of oxygen, the temperature, and the component of the flow velocity normal to the stagnation plane at the oxidizer boundary are represented by $Y_{O_2,2}$, T_2 , and V_2 , respectively. The tangential components of the flow velocities at the boundaries are presumed to be equal to zero. The distance between the fuel boundary and the oxidizer boundary is represented by L . The velocities of the reactants at the boundaries of the counterflow burner are presumed to be equal to the ratio of their volumetric flowrates to the cross-section area of the ducts. The temperature of the fuel stream and the temperature of the oxidizer stream at the boundaries are measured using thermocouples.

The value of the strain rate, defined as the normal gradient of the normal component of the flow velocity, changes from the fuel boundary to the oxidizer boundary [7]. The characteristic strain rate on the oxidizer side of the stagnation plane a_2 is presumed to be given by [7]

$$a_2 = \frac{2|V_2|}{L} \left(1 + \frac{|V_1|\sqrt{\rho_1}}{|V_2|\sqrt{\rho_2}} \right). \quad (1)$$

Here ρ_1 and ρ_2 represent the density of the mixture at the fuel boundary and at the oxidizer boundary, respectively. Equation 1 is obtained from an asymptotic theory where the Reynolds numbers of the laminar flow at the boundaries are presumed to be large [7]. Critical conditions of extinction are presumed to be given by the strain rate, $a_{2,e}$, and the mass fraction of fuel at the fuel boundary. Critical conditions of autoignition are presumed to be given by the strain rate, $a_{2,I}$, the temperature of the oxidizer stream, $T_{2,I}$, and the mass fraction of fuel at the fuel boundary.

The fuels tested were:

- Multicomponent fuels:
 1. JP-8 (obtained from China Lake), JP-8 POSF 4177 (obtained from Wright Patterson Air Force Base (WPAFB)), JP-8 POSF 3773 (obtained from WPAFB).
 2. Jet-A (obtained from San Diego Airport), Jet-A POSF 3602 (obtained from WPAFB), Jet-A POSF 3638 (obtained from WPAFB), Blend POSF 4658.
 3. Fisher Tropesch JP-8 (obtained from WPAFB).

- Fuel mixtures (liquid volume): Possible surrogates of JP-8:
 1. Surrogate A: 60 % *n*-decane, 20 % methylcyclohexane, 20 % toluene. $H/C = 1.93$.
 2. Surrogate B: 60 % *n*-decane, 20 % methylcyclohexane, 20 % *o*-xylene. $H/C = 1.93$.
 3. Surrogate B1: 60 % *n*-decane, 20 % methylcyclohexane, 15 % *o*-xylene, 5 % methyl-naphthalene.
 4. Surrogate C (UCSD surrogate): 60 % *n*-dodecane, 20 % methylcyclohexane, 20 % *o*-xylene. $H/C = 1.92$.
 5. Surrogate C1 : 60 % *n*-dodecane, 20 % methylcyclohexane, 15 % *o*-xylene, 5 % 1-methylnaphthalene.
 6. Surrogate D: *n*-decane 50 %, butylcyclohexane 25 %, butylbenzene 25 %. $H/C = 1.92$.
 7. Surrogate E: *n*-decane 34 %, butylcyclohexane 33 %, butylbenzene 33 %. $H/C = 1.84$.
 8. Surrogate F: *n*-decane 60 %, butylcyclohexane 20 %, butylbenzene 20 %. $H/C = 1.97$.
 9. Aachen Surrogate: *n*-decane 80 %, trimethylbenzene 20 %. $H/C = 1.99$.
 10. Modified Aachen Surrogate: *n*-dodecane 80 %, trimethylbenzene 20 %. $H/C = 1.97$.
 11. Surrogate N1: *n*-decane 80 %, propylbenzene 20 %.
 12. Surrogate N2: *n*-decane 70 %, propylbenzene 30 %.
 13. Drexel Surrogate 1: *n*-dodecane 26 %, iso-cetane 36 %, methylcyclohexane 14 %, decaline 6 %, and 1-methylnaphthalene 18 %. $H/C = 1.82$. [8]
 14. Drexel Surrogate 2: *n*-dodecane 43 %, iso-cetane 27 %, methylcyclohexane 15 %, and 1-methylnaphthalene 15 %. $H/C = 1.87$. [9]
 15. Utah Surrogate: *n*-dodecane 30 %, *n*-tetradecane 20 %, iso-octane 10 %, methylcyclohexane 20 %, *o*-xylene 15 %, and tetraline 5 %. $H/C = 1.93$. [10]
- Fuel Mixtures (liquid volume). Possible surrogate of F-T JP-8.
 1. Surrogate G: *n*-decane 60 %, iso-octane 40 %. $H/C = 2.22$.

3 Extinction of Flames

In the extinction experiments the temperature of the fuel stream is 473 (± 10) K, and the temperature of the oxidizer stream, is 298 K. The distance between the fuel duct and the oxidizer duct is 10 mm. At some selected value of the mass fraction of fuel, $Y_{F,1}$, the flame is stabilized at a strain rate $a_2 < a_{2,e}$, where $a_{2,e}$ is the strain rate at extinction. The strain rate is increased until extinction is observed. The accuracy of the strain rate is $\pm 10\%$ of recorded value and that of the fuel mass fraction $\pm 3\%$ of recorded value. The experimental repeatability on reported strain rate is $\pm 5\%$ of recorded value.

Figure 2 shows experimental data for jet fuels. Extinction characteristics of different batches of JP-8 and different batches of Jet-A are similar. F-T JP-8 is harder to extinguish. Figures 3 and

4 compare experimental extinction data for potential surrogates of JP-8 with that for JP-8. The extinction characteristics of the surrogates are placed in three groups: Group 1 best, Group 2 good, Group 3 significant differences. The surrogates placed in these groups are:

- Group 1: Drexel Surrogate 2, Utah Surrogate, Aachen Surrogate, and Modified Aachen Surrogate.
- Group 2: Surrogate C, Surrogate C1, Surrogate B1, and Surrogate E.
- Group 3: Surrogate D, Surrogate F, Surrogate B, and Surrogate A.

Figure 5 shows that the extinction characteristics of surrogate G agrees well with those for F-T JP-8.

4 Autoignition of Flames

The parameters that influence autoignition are:

1. Composition of the fuel stream, $Y_{F,1}$
2. Temperature of the fuel stream, T_1
3. Composition of the oxidizer stream, $Y_{O_2,2}$
4. Temperature of the oxidizer stream, T_2
5. Strain rate a_2
6. Pressure, p

The experiments are conducted at $T_1 = 473$ K, $Y_{O_2,2} = 0.23$ (air), $p = 1.013$ bar. Two sets of measurements were obtained. In one set the value of $Y_{F,1}$ was maintained at a constant value of 0.4. the values of T_2 were measured for various values of a_2 . In the other set a_2 was maintained at a constant value of 550 s⁻¹. Here the value of T_2 was measured for various values of $Y_{F,1}$. The experimental accuracy of the measured value of T_2 is ± 30 K and that of a_2 is ± 7 % of recorded value, and $Y_{F,1}$ is ± 3 % of recorded value. The experimental uncertainty (repeatability) for T_2 is ± 4 K of recorded value for a given mass fraction of fuel. The transient autoignition process, at any critical condition, was observed using a high speed camera. Only data where autoignition takes place around the axis of symmetry was recorded. Figure 6 shows photographs of the transient autoignition process recorded by a high-speed camera. The fuel is JP-8 with $a_2 = 427$ s⁻¹, $Y_{F,1} = 0.4$, $T_1 = 483$ K, $Y_{O_2,2} = 0.23$, and $T_2 = 1225$ K. The image on the left shows a faint illumination around the axis of symmetry. This is onset of autoignition. The image on the right shows a steady flame.

Figure 7 compares the critical conditions of autoignition of JP-8, Jet-A and F-T JP-8. It shows that the autoignition characteristics of JP-8 and Jet-A are similar, while F-T JP-8 is easier to ignite.

Figures 8 and 9 show that the autoignition characteristics of different batches of JP-8 are the same. Similar results for Jet-A are shown by Figures 10 and 11.

Figures 12, 13, 14 and 15 compare experimental autoignition data for potential surrogates of JP-8 with that for JP-8. The autoignition characteristics of the surrogates are placed in three groups: Group 1 best, Group 2 good, Group 3 significant differences. The surrogates placed in these groups are

- Group 1: Aachen Surrogate.
- Group 2: Surrogate C, Surrogate C1, Surrogate B1, Drexel Surrogate 2, and Modified Aachen Surrogate, Utah Surrogate,
- Group 3: Surrogate D, Surrogate N1, Surrogate N2.

Figures 16 and 17 show that the autoignition characteristics of surrogate G agrees well with those for F-T JP-8.

4.1 Summary

The surrogates of JP-8 are ranked employing the following criteria listed in the order of importance: (1) how well they reproduce critical conditions of autoignition, (2) how close is the hydrogen to carbon ratio to that of JP-8, (3) simplicity (availability of chemical kinetic mechanisms), and (4) how well they reproduce critical conditions of extinction. Using this criteria the surrogates are listed in the following order:

1. Aachen Surrogate,
2. Surrogate C, Surrogate C1, Surrogate B1.
3. Drexel Surrogate 2, and Modified Aachen Surrogate.

The Aachen Surrogate has a H/C ratio of 1.99. Its autoignition characteristics agrees best with JP-8 when compared to all surrogates tested here. Its extinction characteristics agrees well with JP-8. Professor Peters at RWTH Aachen, Germany has measured the volume of soot formed and it is similar to those for JP-8. The Aachen surrogate has only two components. The chemical kinetic mechanism for *n*-decane is well known (Bikas and Peters C&F 126, 1456, 2001). There is a need to compare the low and intermediate temperature chemistry of this surrogate with those for JP-8.

Surrogate C (also called the UCSD surrogate) has H/C ratio of 1.92. This is very close to that of JP-8. The components in the surrogate match the classes of fuel in JP-8. Its autoignition characteristics agrees very well with JP-8. Its extinction characteristics agrees with JP-8, although some differences are observed. It has only three components. Many investigators are developing chemical kinetic mechanisms for the components. There is a need to compare the low and intermediate temperature chemistry of this surrogate with those for JP-8. Surrogates C1 and Surrogate B1

include 1-methylnaphthalene therefore rates of soot production during combustion of these surrogates may be closer to those for JP-8.

The Drexel Surrogate 2 has a H/C ratio is 1.87. Its autoignition characteristics agrees well with JP-8. Its extinction characteristics agrees best with JP-8 in comparison to all surrogates tested. The chemical kinetic mechanisms for the components still are early stages of development. The low and intermediate temperature chemistry of this surrogate agrees well with those for JP-8 (shown by investigators at Drexel).

The Modified Aachen Surrogate has a H/C ratio is 1.97. Very close to that of JP-8. Its autoignition and extinction characteristics agrees well with JP-8. It has only two components. Many investigators are developing chemical kinetic mechanisms for the components. There is a need to compare the low and intermediate temperature chemistry of this surrogate with those for JP-8.

Overall the Aachen surrogate and Surrogate C (UCSD surrogate) appear to best reproduce the combustion characteristics of JP-8. Surrogate G reproduces the combustion characteristics of F-T JP-8.

Acknowledgments

The research at the University of California at San Diego was supported by the U. S. Army Research Office, grant # W911NF-04-1-0139. Program manager Dr. Ralph A. Anthenien Jr, PhD, PE.

References

- [1] In J. W. Hudgens, editor, *Workshop on Combustion Simulation Databases for Real Transportation Fuels*. NIST Gaithersburg, Maryland, September 2003.
- [2] E. Ranzi, T. Faravelli, A. Frassoldati, and S. Granata. *IEC*, 44 (2005) 5170–5183.
- [3] T. Edwards and L. Q. Maurice. *Journal of Propulsion and Power*, 17 (2001) 461–466.
- [4] T. Edwards. *2001 Fall Technical Meeting, Eastern States Section of the Combustion Institute*, (2001) journal.
- [5] R. Seiser, L. Truett, D. Trees, and K. Seshadri. *Proceedings of the Combustion Institute*, 27 (1998) 649–657.
- [6] R. Seiser, K. Seshadri, E. Piskernik, and A. Liñán. *Combustion and Flame*, 122 (2000) 339–349.
- [7] K. Seshadri and F. A. Williams. *International Journal of Heat and Mass Transfer*, 21 (1978) 251–253.
- [8] A. Agosta, N. P. Cernansky, D. L. Miller, T. Faravelli, and E. Ranzi. *Experimental Thermal and Fluid Science*, 28 (2004) 701–708.
- [9] N.P. Cernansky. personal communication, 2006.
- [10] A. Violi, S. Yan, E. G. Eddings, A. F. Sarofim, S. Granata, T. Faravelli, and E. Ranzi. *Combustion Science and Technology*, 174 (2002) 399–417.

List of Figures

- 1 Schematic illustration of the experimental setup. The figure shows the counterflow flow field and the air, nitrogen, and fuel feed systems and the vaporizer. 9
- 2 The mass fraction of fuel as a function of the strain rate at extinction. The symbols represent experimental data, and the lines are best fits to experimental data. The figure compares extinction characteristics of various batches of JP-8, Jet-A, and FT JP-8. 10
- 3 The mass fraction of fuel as a function of the strain rate at extinction. The symbols represent experimental data, and the lines are best fits to experimental data. The figure compares extinction characteristics of various surrogates of JP-8. 10
- 4 The mass fraction of fuel as a function of the strain rate at extinction. The symbols represent experimental data, and the lines are best fits to experimental data. The figures compares extinction characteristics of different UCSD surrogates. 11
- 5 The mass fraction of fuel as a function of the strain rate at extinction. The symbols represent experimental data, and the lines are best fits to experimental data. The figure compares extinction characteristics of a surrogate and FT JP-8. 11
- 6 High speed photograph of onset of autoignition. The fuel is JP-8 with $a_2 = 427 \text{ s}^{-1}$, $Y_{F,1} = 0.4$, $T_1 = 483 \text{ K}$, $Y_{O_2,2} = 0.23$, and $T_2 = 1225 \text{ K}$ 12
- 7 The temperature of the oxidizer stream at autoignition as a function of the strain rate at fixed values of $Y_{F,1} = 0.4$. The symbols are experimental data. The lines are best fit. The figure compares of autoignition characteristics of JP-8, Jet-A, and F-T JP-8 12
- 8 The temperature of the oxidizer stream at autoignition as a function of the strain rate at fixed values of $Y_{F,1} = 0.4$. The symbols are experimental data. The lines are best fit. The figure compares of autoignition characteristics of various batches of JP-8. 13
- 9 The temperature of the oxidizer stream at autoignition as a function of the mass fraction of fuel in the fuel stream, $Y_{F,1}$ at a fixed value of the strain rate $a_2 = 550 \text{ s}^{-1}$. The symbols are experimental data. The lines are best fit. The figure compares of autoignition characteristics of various batches of JP-8. 13
- 10 The temperature of the oxidizer stream at autoignition as a function of the strain rate at fixed values of $Y_{F,1} = 0.4$. The symbols are experimental data. The lines are best fit. The figure compares of autoignition characteristics of various batches of Jet-A. 14
- 11 The temperature of the oxidizer stream at autoignition as a function of the mass fraction of fuel in the fuel stream, $Y_{F,1}$ at a fixed value of the strain rate $a_2 = 550 \text{ s}^{-1}$. The symbols are experimental data. The lines are best fit. The figure compares of autoignition characteristics of various batches of Jet-A. 14

- 12 The temperature of the oxidizer stream at autoignition as a function of the strain rate at fixed values of $Y_{F,1} = 0.4$. The symbols are measurements. The lines are best fit. The figures compares autoignition characteristics of various surrogates of JP-8. 15
- 13 The temperature of the oxidizer stream at autoignition as a function of the mass fraction of fuel in the fuel stream, $Y_{F,1}$ at a fixed value of the strain rate $a_2 = 550 \text{ s}^{-1}$. The symbols are measurements. The lines are best fit. The figures compares autoignition characteristics of various surrogates of JP-8. 15
- 14 The temperature of the oxidizer stream at autoignition as a function of the strain rate at fixed values of $Y_{F,1} = 0.4$. The symbols are measurements. The lines are best fit. The figures compares autoignition characteristics of different UCSD surrogates. 16
- 15 The temperature of the oxidizer stream at autoignition as a function of the mass fraction of fuel in the fuel stream, $Y_{F,1}$ at a fixed value of the strain rate $a_2 = 550 \text{ s}^{-1}$. The symbols are measurements. The lines are best fit. The figures compares autoignition characteristics of different UCSD surrogates. 16
- 16 The temperature of the oxidizer stream at autoignition as a function of the strain rate at fixed values of $Y_{F,1} = 0.4$. The symbols are measurements. The lines are best fit. The figures compares autoignition characteristics of a surrogate of F-T JP-8 17
- 17 The temperature of the oxidizer stream at autoignition as a function of the mass fraction of fuel in the fuel stream, $Y_{F,1}$ at a fixed value of the strain rate $a_2 = 550 \text{ s}^{-1}$. The symbols are measurements. The lines are best fit. The figures compares autoignition characteristics of a surrogate of F-T JP-8 17

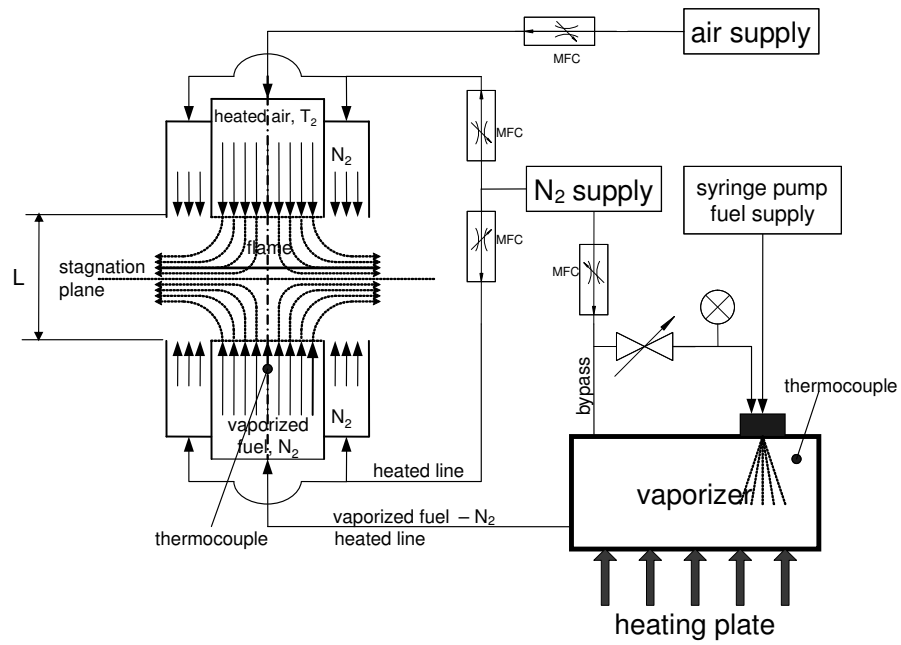


Figure 1: Schematic illustration of the experimental setup. The figure shows the counterflow flow field and the air, nitrogen, and fuel feed systems and the vaporizer.

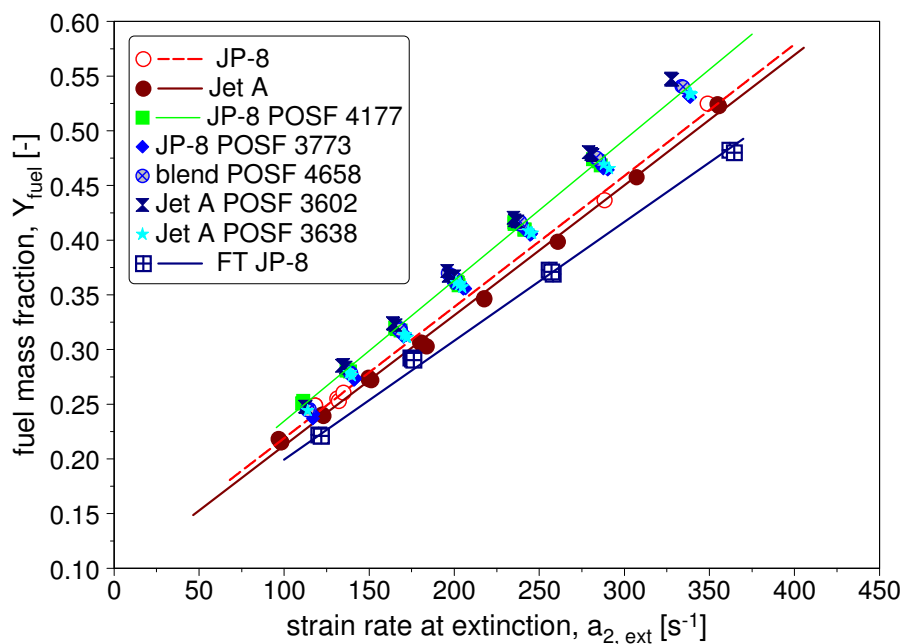


Figure 2: The mass fraction of fuel as a function of the strain rate at extinction. The symbols represent experimental data, and the lines are best fits to experimental data. The figure compares extinction characteristics of various batches of JP-8, Jet-A, and FT JP-8.

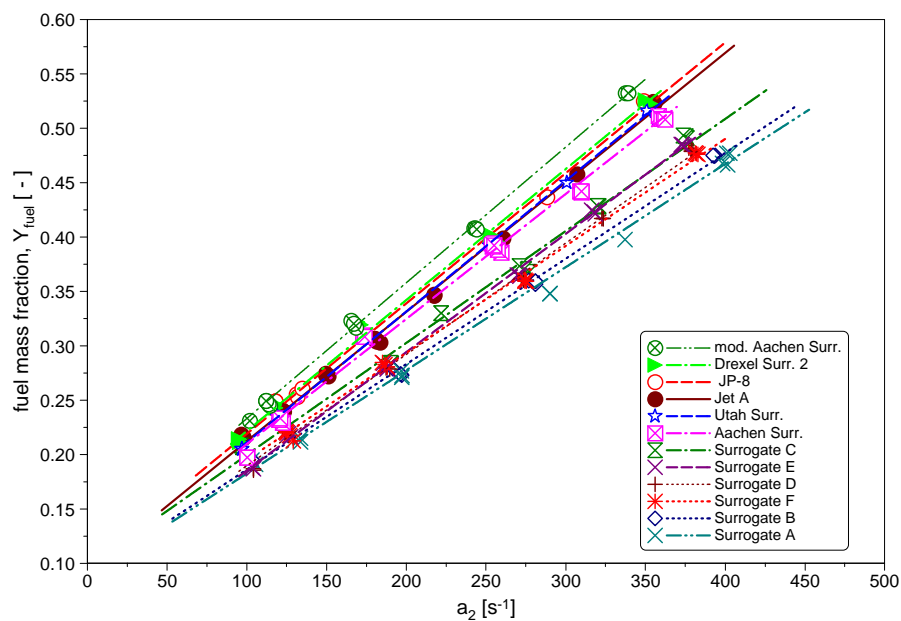


Figure 3: The mass fraction of fuel as a function of the strain rate at extinction. The symbols represent experimental data, and the lines are best fits to experimental data. The figure compares extinction characteristics of various surrogates of JP-8.

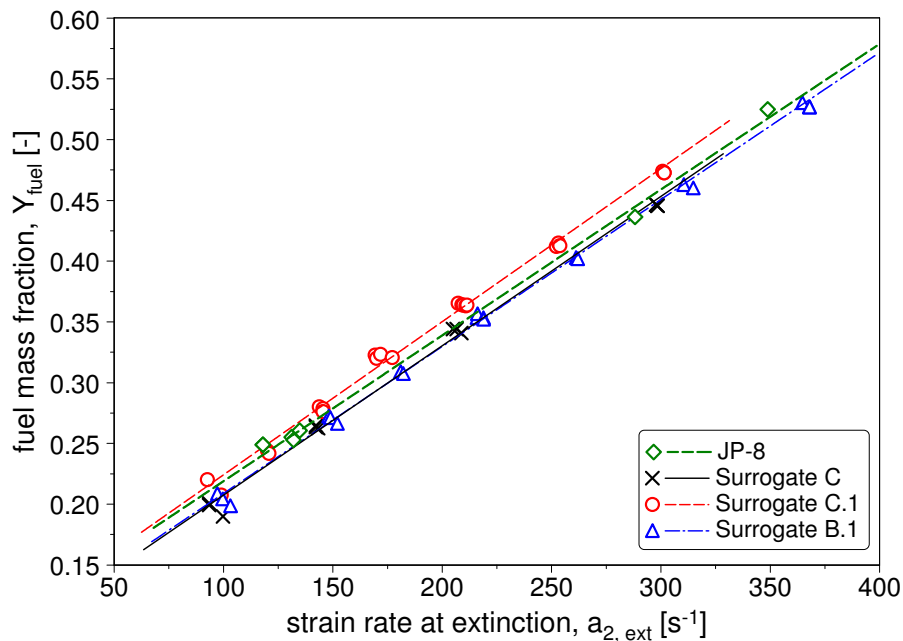


Figure 4: The mass fraction of fuel as a function of the strain rate at extinction. The symbols represent experimental data, and the lines are best fits to experimental data. The figures compares extinction characteristics of different UCSD surrogates.

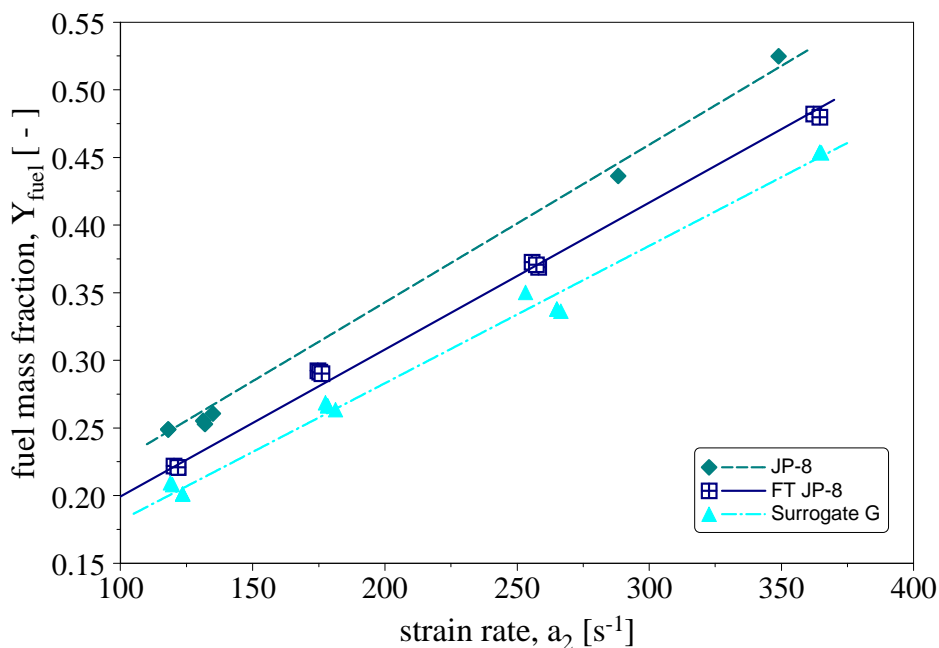


Figure 5: The mass fraction of fuel as a function of the strain rate at extinction. The symbols represent experimental data, and the lines are best fits to experimental data. The figure compares extinction characteristics of a surrogate and FT JP-8.

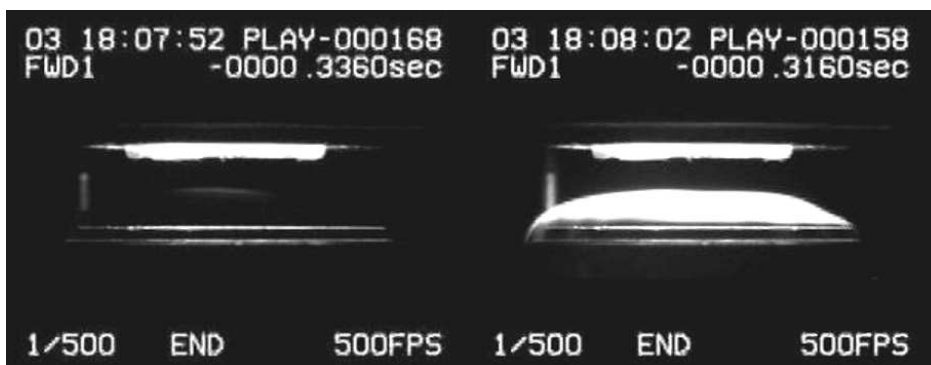


Figure 6: High speed photograph of onset of autoignition. The fuel is JP-8 with $a_2 = 427 \text{ s}^{-1}$, $Y_{F,1} = 0.4$, $T_1 = 483 \text{ K}$, $Y_{O_2,2} = 0.23$, and $T_2 = 1225 \text{ K}$.

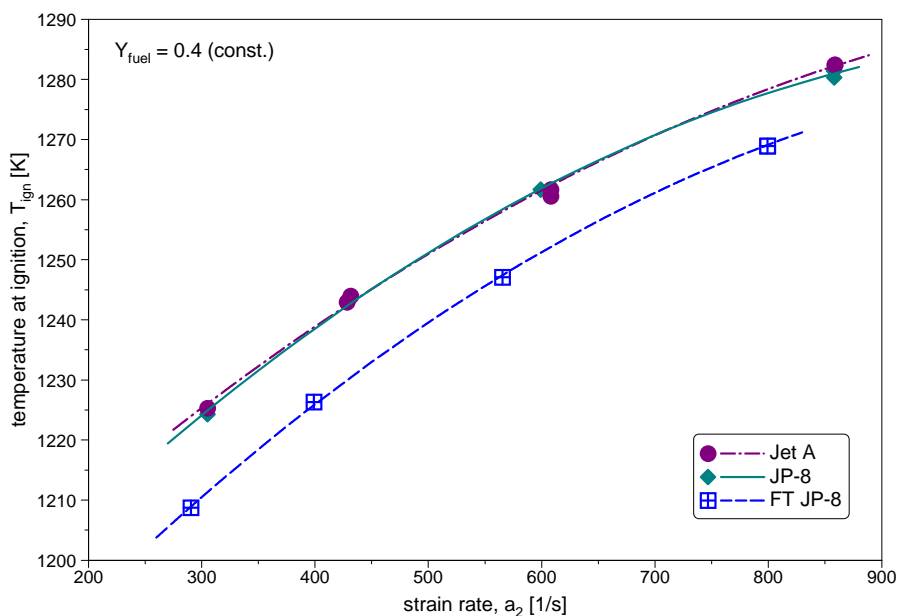


Figure 7: The temperature of the oxidizer stream at autoignition as a function of the strain rate at fixed values of $Y_{F,1} = 0.4$. The symbols are experimental data. The lines are best fit. The figure compares of autoignition characteristics of JP-8, Jet-A, and F-T JP-8

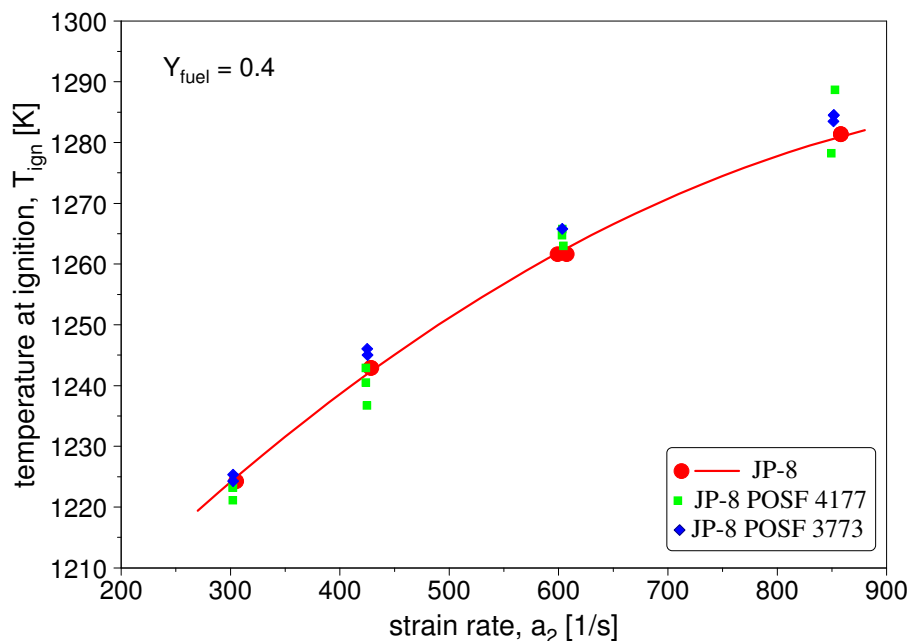


Figure 8: The temperature of the oxidizer stream at autoignition as a function of the strain rate at fixed values of $Y_{F,1} = 0.4$. The symbols are experimental data. The lines are best fit. The figure compares of autoignition characteristics of various batches of JP-8.

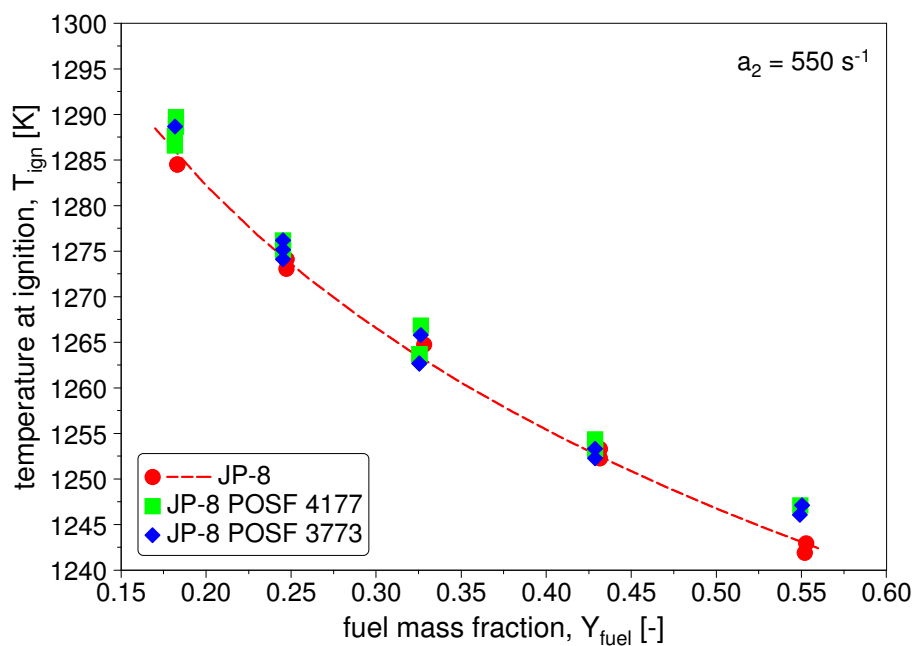


Figure 9: The temperature of the oxidizer stream at autoignition as a function of the mass fraction of fuel in the fuel stream, $Y_{F,1}$ at a fixed value of the strain rate $a_2 = 550 \text{ s}^{-1}$. The symbols are experimental data. The lines are best fit. The figure compares of autoignition characteristics of various batches of JP-8.

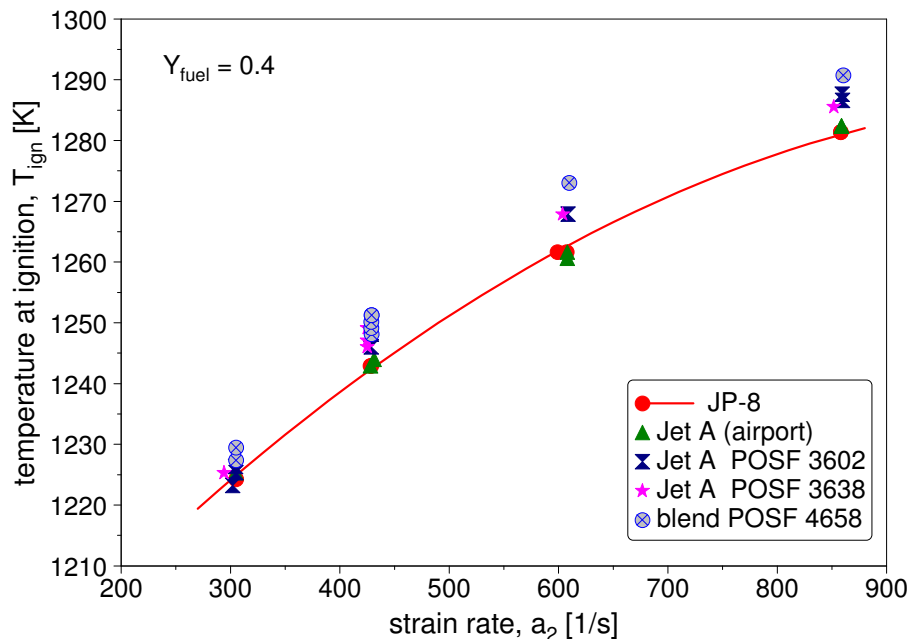


Figure 10: The temperature of the oxidizer stream at autoignition as a function of the strain rate at fixed values of $Y_{F,1} = 0.4$. The symbols are experimental data. The lines are best fit. The figure compares of autoignition characteristics of various batches of Jet-A.

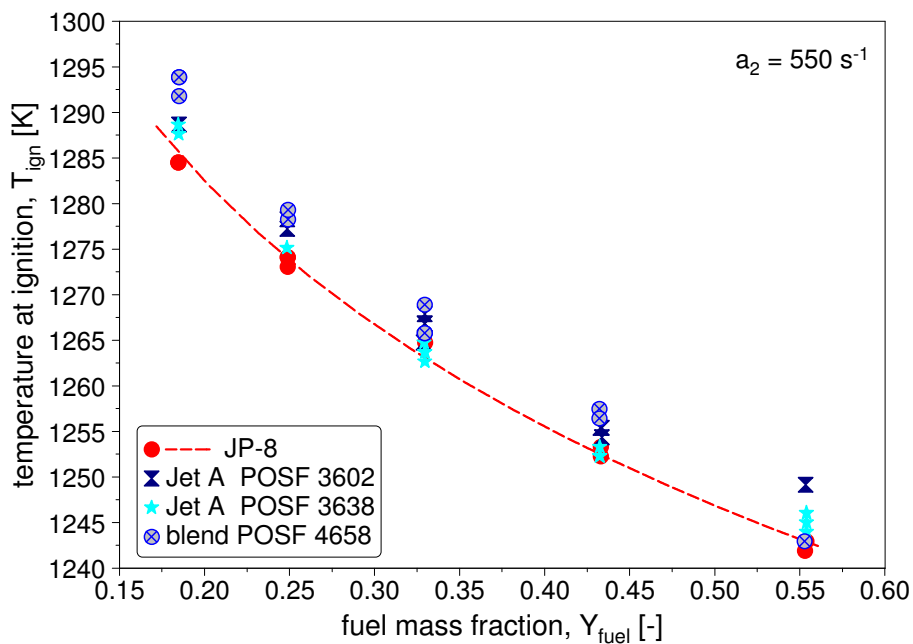


Figure 11: The temperature of the oxidizer stream at autoignition as a function of the mass fraction of fuel in the fuel stream, $Y_{F,1}$ at a fixed value of the strain rate $a_2 = 550 \text{ s}^{-1}$. The symbols are experimental data. The lines are best fit. The figure compares of autoignition characteristics of various batches of Jet-A.

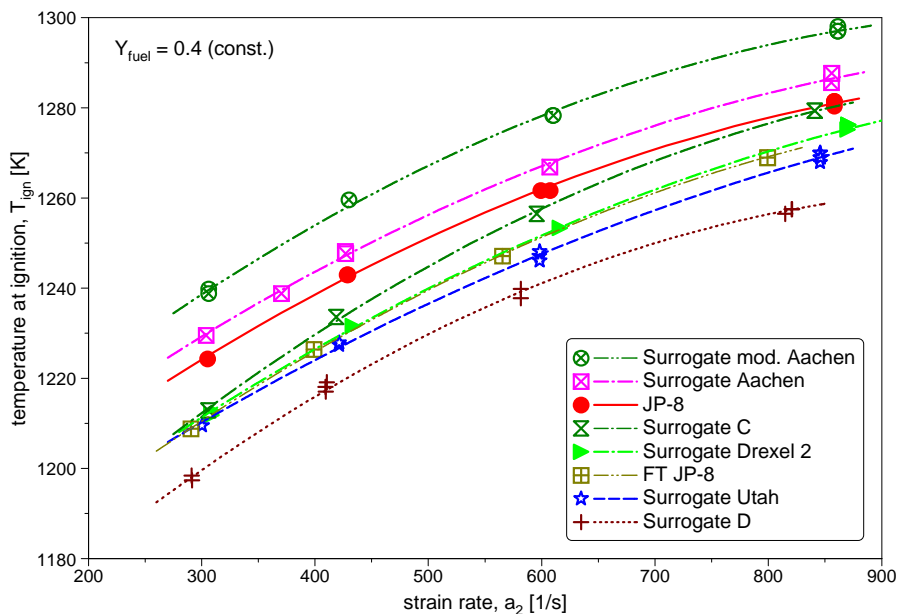


Figure 12: The temperature of the oxidizer stream at autoignition as a function of the strain rate at fixed values of $Y_{F,1} = 0.4$. The symbols are measurements. The lines are best fit. The figures compares autoignition characteristics of various surrogates of JP-8.

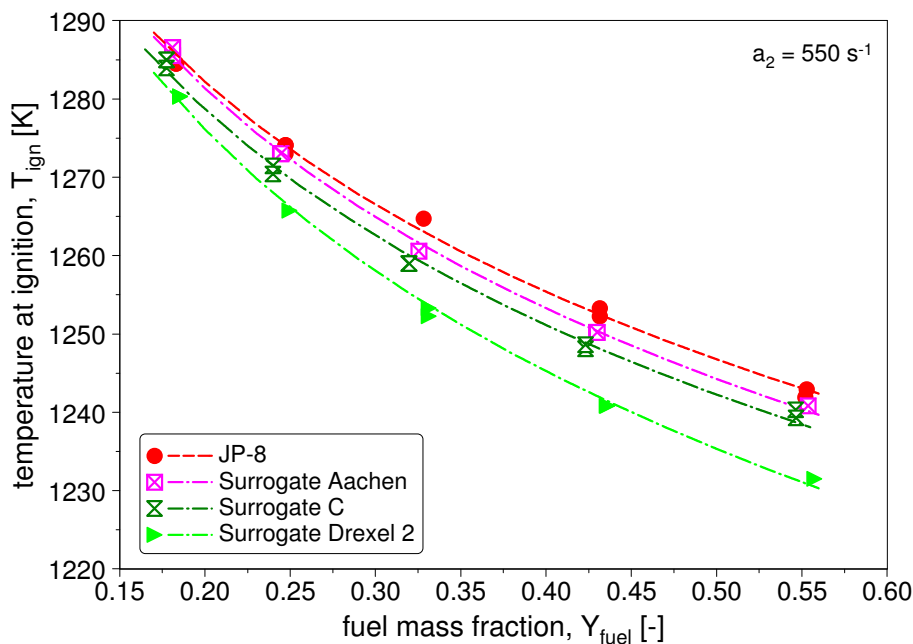


Figure 13: The temperature of the oxidizer stream at autoignition as a function of the mass fraction of fuel in the fuel stream, $Y_{F,1}$ at a fixed value of the strain rate $a_2 = 550 \text{ s}^{-1}$. The symbols are measurements. The lines are best fit. The figures compares autoignition characteristics of various surrogates of JP-8.

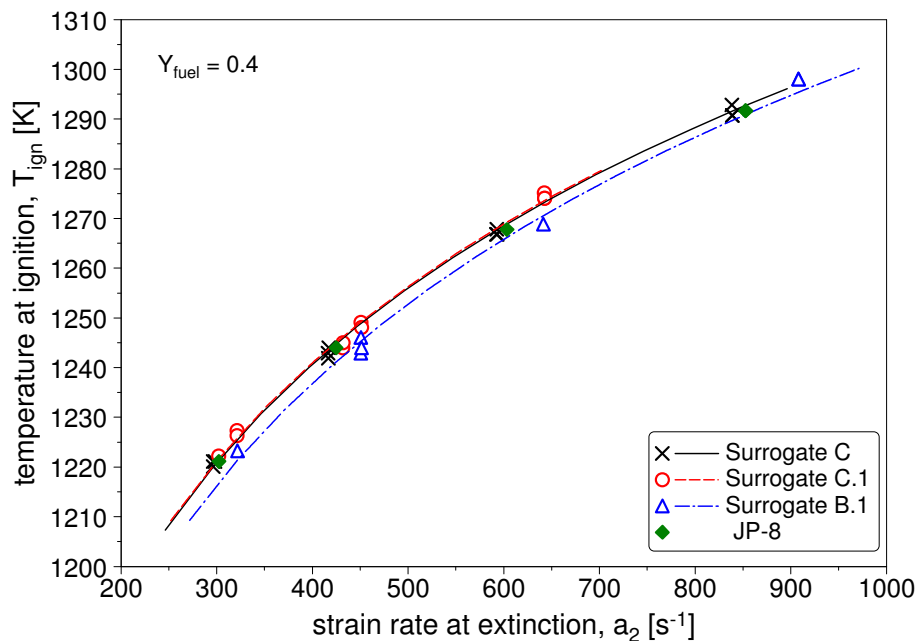


Figure 14: The temperature of the oxidizer stream at autoignition as a function of the strain rate at fixed values of $Y_{F,1} = 0.4$. The symbols are measurements. The lines are best fit. The figures compares autoignition characteristics of different UCSD surrogates.

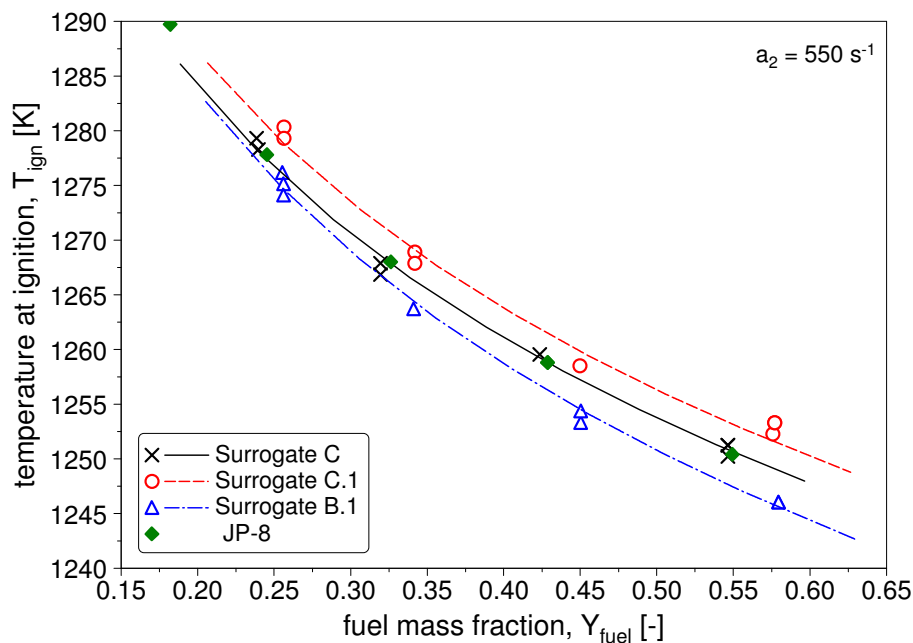


Figure 15: The temperature of the oxidizer stream at autoignition as a function of the mass fraction of fuel in the fuel stream, $Y_{F,1}$ at a fixed value of the strain rate $a_2 = 550 \text{ s}^{-1}$. The symbols are measurements. The lines are best fit. The figures compares autoignition characteristics of different UCSD surrogates.

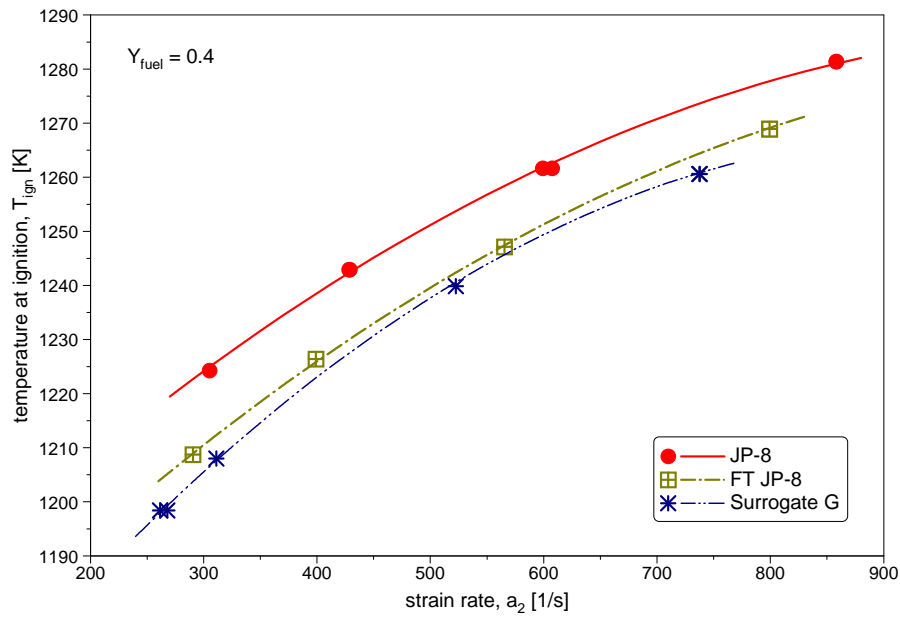


Figure 16: The temperature of the oxidizer stream at autoignition as a function of the strain rate at fixed values of $Y_{F,1} = 0.4$. The symbols are measurements. The lines are best fit. The figures compares autoignition characteristics of a surrogate of F-T JP-8

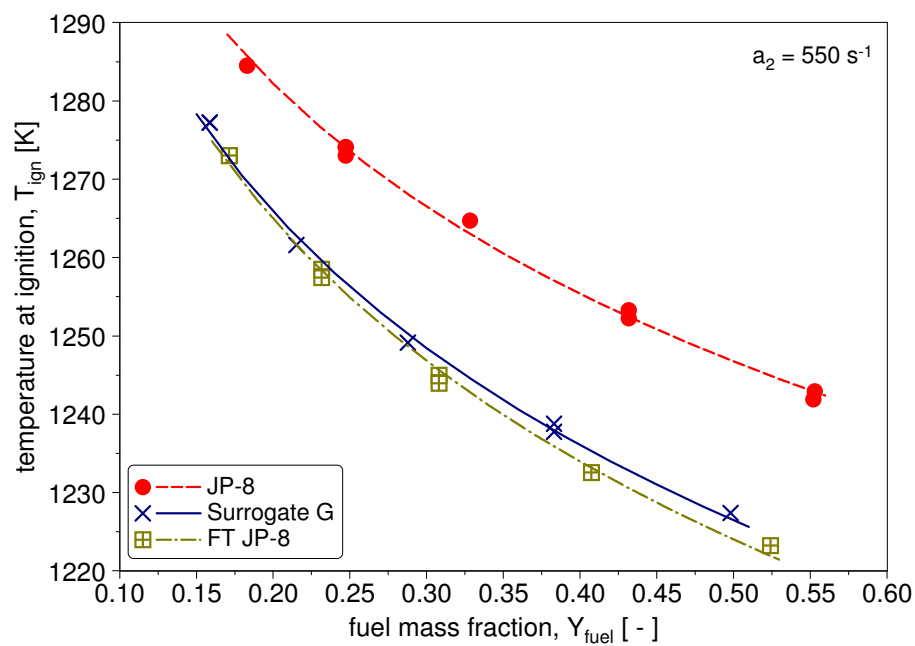


Figure 17: The temperature of the oxidizer stream at autoignition as a function of the mass fraction of fuel in the fuel stream, $Y_{F,1}$ at a fixed value of the strain rate $a_2 = 550 \text{ s}^{-1}$. The symbols are measurements. The lines are best fit. The figures compares autoignition characteristics of a surrogate of F-T JP-8

Appendix A

Here we describe tests carried out to prove that no decomposition of Jet-A and JP-8 takes place in the fuel lines of our counterflow burner. A schematic illustration of the counterflow configuration is shown in Fig. A1.

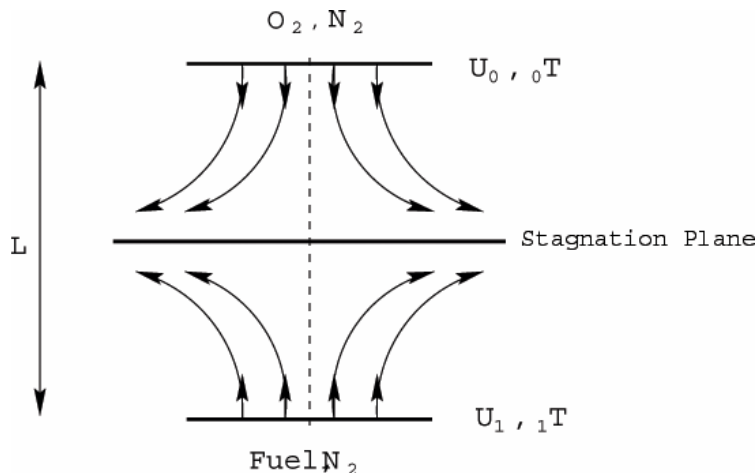


Figure A1: Schematic illustration of the counterflow configuration

The counterflow burner is made up of two ducts. Here, a fuel stream made up of prevaporized fuel and nitrogen is injected from one duct, and an oxidizer stream made up of oxygen and nitrogen is injected from the other duct. The velocities of the fuel stream and the oxidizer stream at the injection planes are represented by U_1 and U_0 , respectively. The temperatures of the fuel stream and the oxidizer stream at the injection planes are represented by T_1 and T_2 , respectively. The distance between the injection planes is L . The liquid fuels are vaporized in a device called a multicomponent vaporizer. This device has a heated mixing chamber into which fuel is sprayed as a fine mist together with nitrogen. To prevent condensation, the vaporizer and flow lines are heated. The temperature of fuel vapors entering the counterflow burner is measured using a thermocouple.

Experiments were performed to verify that jet-fuel did not decompose, when its vapors are carried in hot nitrogen towards the burner. For this purpose, the apparatus was modified in a way, that a line was attached to the exit of the fuel-duct, followed by a condenser and an aerosol filter. The modified apparatus is shown in Fig. A2. The purpose was to re-condense the fuel vapors and analyze the resulting liquid in a massspectrometer. The vapors that remained in the nitrogen stream after the aerosol filter were analyzed in a gas-chromatograph.

The conditions for this experiment are described in the following. The fuel side velocity is 0.375 m/s with an approximately equal curtain co-flow velocity. The mass fraction of fuel in the fuel stream is 0.228 with the balance being nitrogen. This corresponds to an oxidizer strain rate of 128 s^{-1} for the counterflow setup. The temperatures of the apparatus components on the fuel-side were measured using thermocouples. The temperature of the vaporizer was 513 K, the

temperature at the exit of the fuel-duct was 493 K, and the flow lines in between had various temperatures with a local maximum of 563 K.

After the portions of jet-fuel were collected in the condenser and the aerosol filter, a liquid sample was created by mixing the two portions together in approximately the same ratio as they were collected in the two units. A reference sample was taken from the original jet-fuel. The two samples were analyzed in a gas-chromatograph/massspectrometer.

Figure A3 shows the comparison of the two samples. The total mass count of the mass-selective detector is plotted versus the time it takes for a component to travel through the GC-column and reach the detector. The black result represents the original jet-fuel and the red result represents the jet-fuel that was vaporized, heated, and recondensed. It can be seen from these results, that the chromatograms are nearly identical, and that there is no major shift from any major fuel groups to others. Most peaks are preserved and have about equal height between the two samples, that is, within the accuracy of the instrument. The differences between the two samples are also smaller than when two different jet-fuels are compared. Figure A4 shows a comparison between Jet-A purchased at local airport (Montgomery Field, no pristine added) and Jet-A received from WPAFB, shown in black and blue, respectively. At last, Fig. A5 shows a comparison between Jet-A and JP-8 (WPAFB). In Figs. 4 and 5 it can be seen that the same major components, as indicated by large peaks, are present within the different fuels. The amounts, as indicated by the height of the peaks are sometimes smaller or larger between the different fuels. In summary, the jet-fuel that has been used in the vaporizer shows less variation from the original fuel than different jet-fuels vary from each other.

A second test was performed to test if there were any smaller hydrocarbon species created by thermal breakdown of the fuel in the vaporizer. These species would not be detected in the GC-MS system, which is limited to species with molecular weight of above ca. 100. Some of these species could be condensed out in the condenser/filter, others could leave the system as vapors. A gas-chromatograph was used to monitor these gases/vapors (see Fig. A2). A GC-column combination of a molesieve and a Porapaq Q column was used to separate the species, and a flame-ionization-detector (FID) was used to detect them. A sampling line was connected from the end of the flow arrangement to the sample-loop in the gas-chromatograph. To measure components already present and dissolved in the original jet-fuel, a liquid sample (0.002 ml) was injected with a syringe into the instrument's injection port. The chromatograms of both analyses are shown in Fig. A6. There are four peaks easily identified in the chromatogram of the exit-gas (red line). When compared with the reference (black line) it is seen, that all four components are also present in the original fuel. The relative amounts are also consistent, since it is expected that more volatile species (peaks toward the left) are enriched in the exit-gas compared to less volatile species (peaks toward the right), since the vaporization and condensation in effect represent a distillation step. In summary, no new species (that could be products of fuel breakdown) were detected in the analysis of the vapors leaving the experiment. These experiments clearly prove that the jet-fuels do not decompose in the fuel lines.

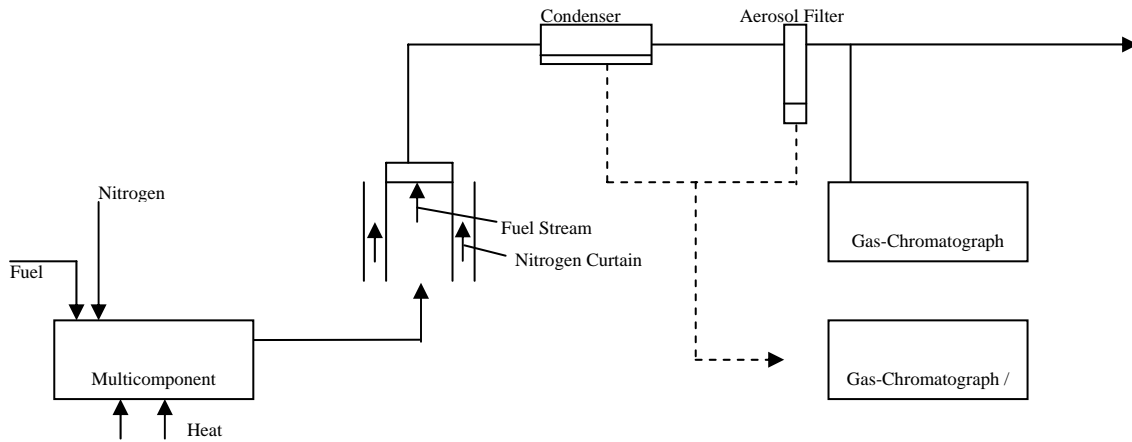


Figure A2: Schematic illustration of the experimental setup.

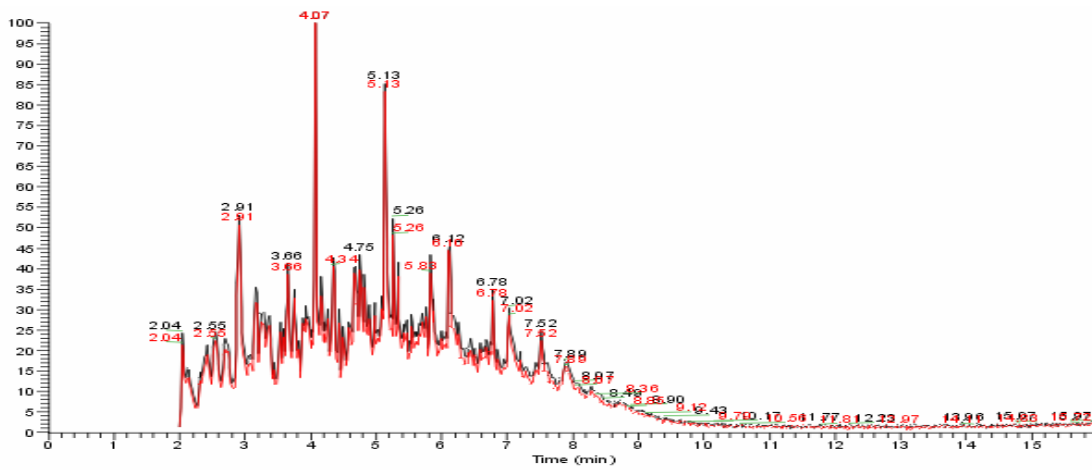


Figure A3: GC-MS output of jet-fuel. The black curve represents the original jet-fuel. The red curve represents the jet-fuel after it was vaporized and recondensed.

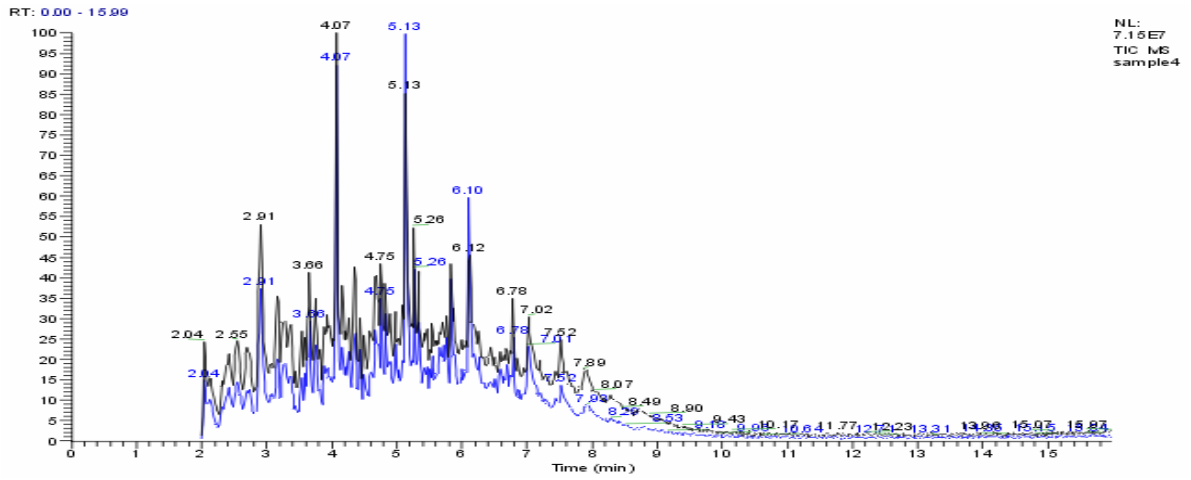


Figure A4: GC-MS output of Jet-A fuels. The black curve represents the original jet-fuel purchased at a local airport. The blue curve represents jet-fuel from WPAFB.

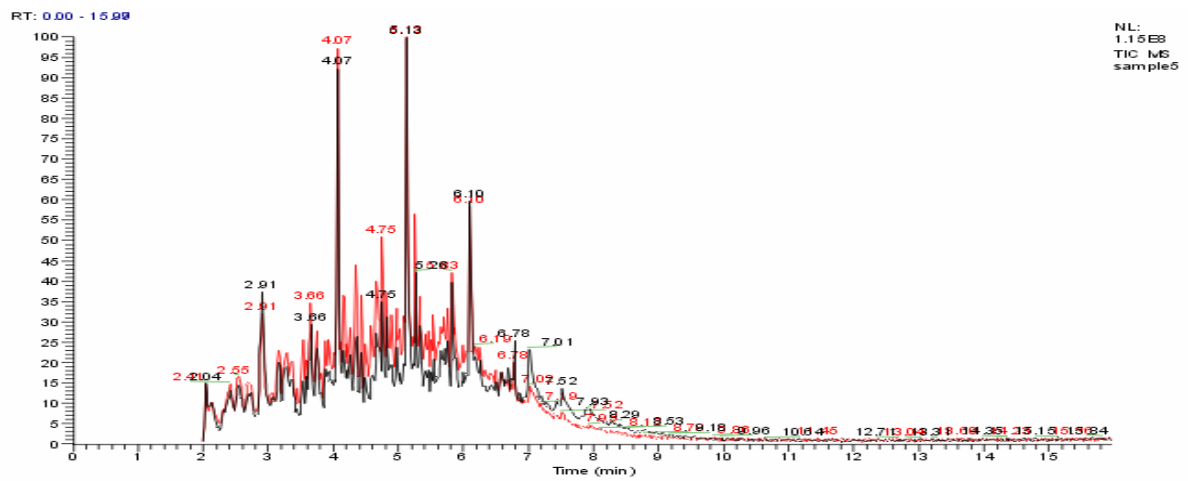


Figure A5: GC-MS output of jet-fuels. The black curve represents Jet-A from WPAFB. The red curve represents JP-8 from WPAFB.

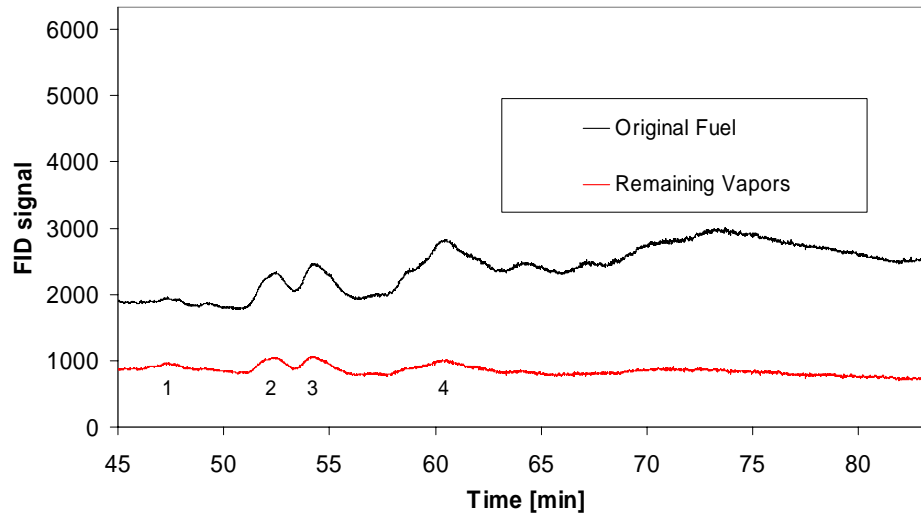


Figure A6: GC output of jet-fuel liquid and vapor fraction. The black curve represents original Jet-A injected as a liquid. The red curve represents the portion of the vaporized fuel that was not captured in the condenser and aerosol filter.

5th US Combustion Meeting
Organized by the Western States Section of the Combustion Institute
and Hosted by the University of California at San Diego
March 25-28, 2007.

Autoignition and Extinction of Methyl-Esters in Nonpremixed Flows

*Ulrich Niemann*¹, *Justin Gerritzen*², *Reinhard Seiser*³,
*Stefan Humer*¹ and *Kalyanasundaram Seshadri*¹

¹*Department of Mechanical and Aerospace Engineering,
University of California at San Diego, La Jolla, California 92093-0411, USA*

²*Technische Universiteit Eindhoven,
Eindhoven, The Netherlands*

³*Oryxe Energy International, Inc.
Irvine, California*

Biodiesel is defined as mono-alkyl esters of long chain fatty acids derived from vegetable oils. It contains no petroleum, but it can be blended at any level with petroleum diesel to create a biodiesel blend. An improved understanding of the combustion characteristics of esters can provide insights on combustion of biodiesel. Critical conditions of extinction and autoignition are measured for diesel, biodiesel and a number of esters in nonuniform flow fields under nonpremixed conditions. The esters considered are methyl butanoate, methyl crotonate, and ethyl propionate. Methyl butanoate is considered to be a surrogate for biodiesel. The counterflow configuration is employed. The strain rate at extinction is measured as a function of the composition of the reactant streams of the counterflow system. In the autoignition experiments, the temperature of air is increased until autoignition is obtained. The temperature of air at autoignition is measured for various values of strain rate. Numerical calculations are performed using a previously developed chemical-kinetic mechanism for methyl butanoate. The critical conditions of extinction and autoignition calculated using this mechanism is found to agree well with experimental data.

1 Introduction

Biodiesel is a nontoxic alternative fuel produced from renewable resources. In the United States biodiesel is generally made from soybean seeds. Biodiesel from soybean seeds consists of five methyl esters. Their proportions by volume are methyl palmitate (11 %), methyl stearate (4 %) methyl oleate (17 %), methyl linoleate (67 %), methyl linolenate (1 %). Research is in progress in many laboratories to investigate if pollutant emissions can be reduced by addition of biodiesel to diesel [1–4]. Wang et. al [4] measured exhaust emissions from heavy trucks employing as fuel a blend of 65 % diesel and 35 % biodiesel. This blend is called as B35. The emissions were compared with those measured using diesel as fuel [4]. The test results showed that the heavy trucks fueled by B35 emitted significantly lower particulate matter (PM) and moderately lower carbon monoxide (CO) and hydrocarbons (HC) than the same trucks fueled by diesel. Oxides of nitrogen emissions were generally in the same level [4]. This clearly shows that biodiesel has promise as an

emissions-reducing alternative fuel for diesel engines.

An improved understanding of combustion characteristics esters is a first step in understanding the combustion characteristics of biodiesel. Methyl butanoate, for example, is considered as a surrogate for biodiesel fuels [5]. Fisher et. al. [5] have developed a detailed chemical-kinetic model for describing the combustion of methyl butanoate. This mechanism has been tested against limited experimental data that was obtained at low temperatures, sub-atmospheric conditions in closed vessels. These experimental data were obtained in premixed systems and did not include the influence of fluid flow. Here, experimental and numerical studies are carried out on non-premixed combustion of methyl butanoate, methyl crotonate, and ethyl propionate in nonuniform flows. Critical conditions of autoignition and extinction are measured. A detailed chemical-kinetic mechanism for methyl butanoate employed in Ref. [5] is used here to calculate critical conditions of autoignition and extinction in non-premixed flows. The results are compared with experimental data. Critical conditions of autoignition are also measured for diesel (obtained from a local vendor), biodiesel, *n*-heptane, and a mixture of 80 % *n*-heptane and 20 % methyl butanoate by volume. *n*-Heptane is considered as a surrogate for diesel, while methyl butanoate is a surrogate for biodiesel. Thus studies on mixtures of *n*-heptane and methyl butanoate can be used to obtain an improved understanding of the influence of biodiesel on combustion of diesel.

2 Experimental and numerical studies

2.1 Experimental

To capture the influence of the flow field on the critical conditions of autoignition and flame extinction, experiments are conducted in the counterflow configuration. Two types of configuration, the condensed fuel configuration and the prevaporized fuel configuration, are employed. Figure 1 shows a schematic illustration of the condensed fuel configuration. Here, oxidizer is injected

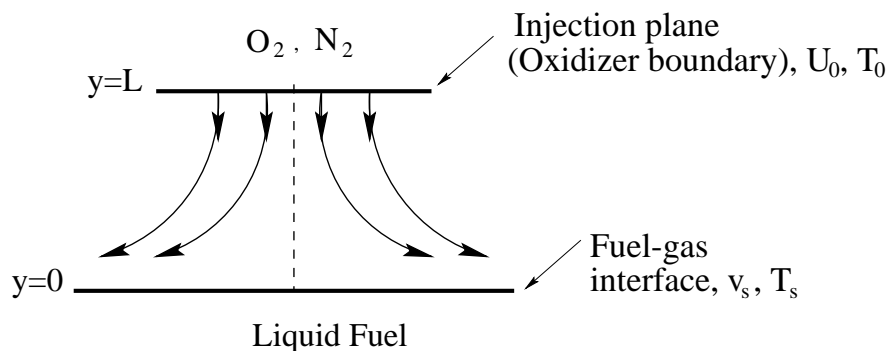


Figure 1: Schematic illustration of the condensed fuel configuration. U_0 and v_s are the velocities at the oxidizer-injection and the gas side of the liquid-gas interface planes, respectively. T_0 and T_s are the temperatures at the oxidizer-injection and the liquid-gas interface planes, respectively.

from a duct and it flows against fuel evaporating from the surface of a liquid pool. The oxidizer is a mixture of oxygen and nitrogen. At the injection plane, the velocity of the oxidizer stream is

denoted by U_0 and the temperature is denoted by T_0 . At the liquid-gas interface, the velocity on the gas side is denoted by v_s and the temperature is denoted by T_s . The distance between the surface of the liquid fuel and the injection plane is L . It has been shown previously that the strain rate is given by [6].

$$a = 2U_0/L. \quad (1)$$

In the condensed fuel configuration, extinction experiments are performed with the temperature oxidizer stream, $T_0 = 298$ K, and the separation distance $L = 10$ mm. At a given value of the mass fraction of oxygen in the oxidizer stream $Y_{O_2,2}$, the velocity of the oxidizer stream is increased until extinction takes place. The strain rate at extinction is calculated using Eqn. (1). It is represented by a_2 . The experiments are repeated at different values of $Y_{O_2,2}$. In the autoignition experiments the oxidizer stream is air and $L = 12$ mm. Here for a given value of the flow velocity of the oxidizer stream, U_0 , its temperature, T_0 is increased until autoignition takes place. The value of T_0 at autoignition is represented by $T_{0,I}$. The value of strain rate is calculated using Eqn. (1). It is represented by a_2 . Values of $T_{0,I}$ are measured for various values of a_2 .

The prevaporized fuel configuration shown in Fig. 2. Here a fuel stream made up of prevaporized

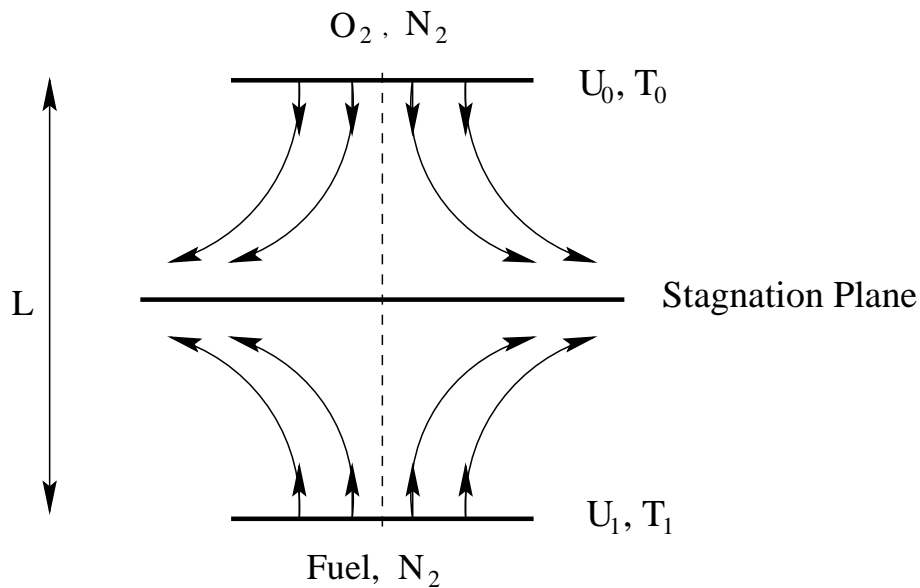


Figure 2: Schematic illustration of the prevaporized fuel configuration. U_0 and T_0 are the velocity and temperature at the oxidizer-injection plane and U_1 and T_1 are the velocity and temperature at the fuel-injection plane.

fuel and nitrogen is injected from one duct and an oxidizer stream made up of oxygen and nitrogen is injected from the other duct. The velocities of the fuel stream and the oxidizer stream at the injection planes are represented by U_1 and U_0 , respectively. The temperatures of the fuel stream and the oxidizer stream at the injection planes are represented by T_1 and T_0 , respectively. The distance between the injection planes is L . The strain rate on the oxidizer side of the stagnation

plane, a is given by the expression [6]

$$a = \frac{2|U_0|}{L} \left(1 + \frac{|U_1|\sqrt{\rho_1}}{|U_0|\sqrt{\rho_0}} \right),$$

where ρ_0 and ρ_1 are, respectively, the density of the oxidizer stream and the fuel stream at the injection planes.

A detailed description of the burner is given elsewhere [7]. In the extinction experiments the temperature of the fuel stream, T_1 , for methyl butanoate, methyl crotonate, and ethyl propionate respectively are 453 (± 10) K, 448 (± 10) K, and 445 (± 10) K. The temperature of the oxidizer stream, $T_0 = 298$ K. The distance between the fuel boundary and the oxidizer boundary is $L = 10$ mm. At some selected value of the mass fraction of fuel in the fuel stream, $Y_{F,1}$, the flame is stabilized. The strain rate is increased by increasing U_1 and U_0 until extinction is observed. The accuracy of the strain rate is $\pm 10\%$ of recorded value and that of the fuel mass fraction $\pm 3\%$ of recorded value. The experimental repeatability on reported strain rate is $\pm 5\%$ of recorded value. In the autoignition experiments the distance between the fuel boundary and the oxidizer boundary is $L = 12$ mm and the mass fraction of fuel in the fuel stream $Y_{F,1} = 0.4$ and the temperature, T_1 , for methyl butanoate, methyl crotonate, and ethyl propionate respectively are 433 (± 10) K, 458 (± 10) K, and 458 (± 10) K. At chosen values of strain rate the flow field is established. The temperature of air is increased until autoignition takes place. The temperature of the oxidizer stream at autoignition, $T_{0,I}$ is recorded as a function of the strain rate. The accuracy of the measurement of the temperature of air at autoignition is expected to be ± 30 K, the strain rate $\pm 10\%$, and fuel mass fraction $\pm 3\%$ of recorded value. The experimental repeatability in the measurement of the temperature of air at autoignition is expected to be ± 6 K.

2.2 Numerical

Numerical computations are performed to predict the critical conditions of extinction and autoignition for methyl butanoate. A computer program called the Flamemaster is used to integrate the conservation equations of mass, momentum and energy, and the species balance equations [8]. The species balance equations include thermal diffusion, and the energy conservation equation includes radiative heat loss from carbon dioxide and water vapor. Buoyancy is neglected. The chemical-kinetic mechanism for methyl butanoate employed in the calculations is derived from the one published by Fisher et al. [5]. At both ends of the computational domain the tangential components of the flow velocity are set to zero (the so-called plug-flow boundary conditions). For the gaseous boundaries, the normal component of the flow velocity, the temperature, and the mass fluxes of species are specified according to the experiments. Here, the flow velocities are calculated from the flow rates divided by the cross-sectional areas. For the liquid boundary in the condensed fuel configuration, the heat of vaporization of the fuel is specified as 331.28 kJ/kg. The mass-flux of the fuel evaporating from the liquid surface is obtained during the numerical computations from an energy balance. Here, the rate of heat conducted to the fuel surface per unit area is equated to the product of the mass burning rate of fuel per unit area and the heat of vaporization. Heat losses from the liquid pool to the burner is neglected. The surface temperature is assumed to

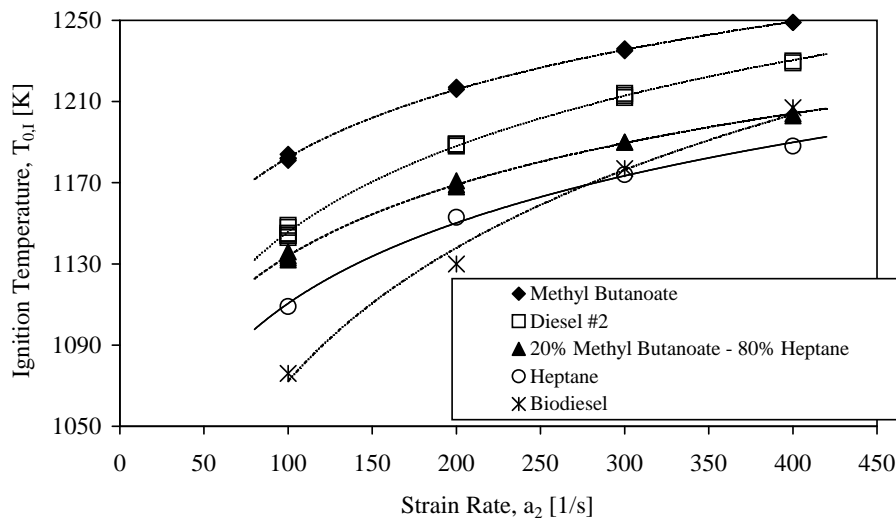


Figure 3: Experimental data showing the temperature of air at autoignition, $T_{0,I}$, as a function of the strain rate. The symbols represent measurements. The lines are best fits to the experimental data. The experimental data was obtained employing the condensed fuel configuration shown in Fig. 1

be the normal boiling point of methyl butanoate. Hence the surface temperature $T_s = 375$ K. To facilitate the numerical computations in the quasi-one dimensional configuration, the mechanism was reduced regarding the number of reactive species. This was done by performing a number of homogeneous reactor (zero dimensional) calculations for different temperatures, pressures, and equivalence ratios. The initial temperatures chosen were 1200 K, 1600 K, and 2000 K. The pressures were 1 and 10 bar, and the equivalence ratios were 1 and 2. Over all combinations of these quantities, ignition delay times were calculated with the full mechanism, and with all mechanisms that had one species at a time removed. Based on the root-mean-square deviation from the ignition delay time of the full mechanism, the mechanism was reduced from 256 to 75 reactive species. Based on a reaction path analysis, 8 more species were eliminated that were only produced but not consumed in this skeletal mechanism. The species C_2H_5OH and CH_3CHCO were eliminated since they were only formed from C_2H_5 and C_3H_6 , respectively, and did not appear to be crucial for the oxidation reactions starting with methyl butanoate. After introducing these simplifications the chemical-kinetic employed in the numerical calculations is made up of 65 reactive species and 415 reversible reactions. This mechanism is used to calculate the critical conditions of extinction and autoignition in the condensed fuel and prevaporized fuel configurations.

3 Experimental Results

Figure 3 shows critical conditions of autoignition for a number of fuels. The experimental data in Fig. 3 was obtained employing the condensed fuel configuration. It shows the temperature of air, $T_{0,I}$, at autoignition as a function of the strain rate, a_2 , for biodiesel, diesel, *n*-heptane, methyl butanoate, a mixture 80 % *n*-heptane and 20 % methyl butanoate by volume. At a given value of the strain rate, a_2 , autoignition will take place for values of the air temperature larger than $T_{0,I}$. For

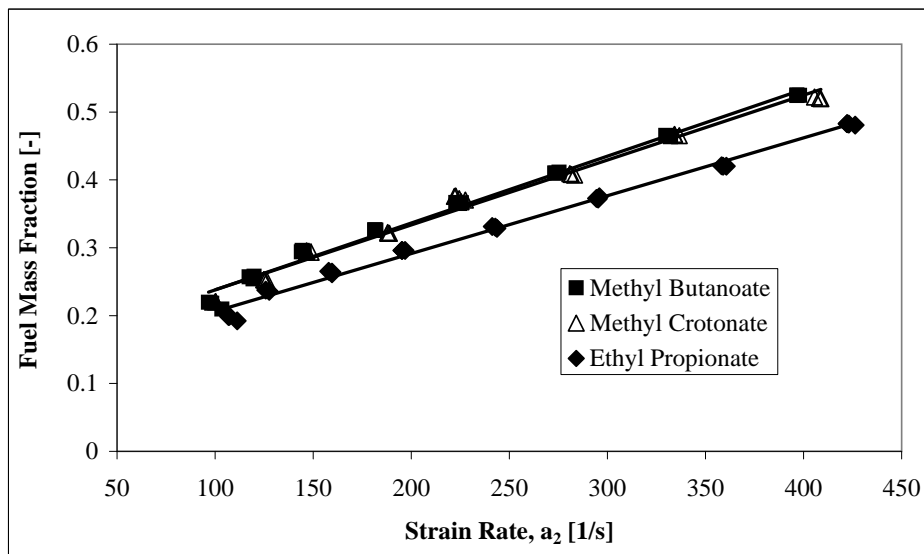


Figure 4: Experimental data showing the mass fraction of fuel in the fuel stream, $Y_{F,1}$, as a function of the strain rate, a_2 , at extinction. The symbols represent measurements. The lines are best fits to the experimental data. The experimental data was obtained employing the prevaporized fuel configuration shown in Fig. 2

all fuels tested the value of $T_{0,I}$ increases with increasing a_2 . It shows that at a fixed value of a_2 , the value of $T_{0,I}$ for methyl butanoate is the highest followed by diesel, the mixture of 80 % *n*-heptane and 20 % methyl butanoate, and *n*-heptane. Therefore among these fuels *n*-heptane is easiest to ignite and methyl butanoate the most difficult to ignite. At low strain rates and biodiesel is easier to ignite when compared with *n*-heptane, while at high strain rate it is more difficult to ignite.

Figure 4 compares the critical conditions of extinction for various esters. The experimental data was obtained using the prevaporized fuel configuration. It shows the mass fraction of fuel in the fuel stream, $Y_{F,1}$ as a function of the strain rate. The critical conditions of extinction of methyl butanoate and methyl crotonate are nearly the same. At a given value of $Y_{F,1}$ the value of a_2 at extinction for ethyl propionate is much larger than that for methyl butanoate and methyl crotonate. Therefore ethyl propionate is much more difficult to extinguish when compared with the other esters. Figure 5 compares the critical conditions of autoignition for the esters. The experimental data in Fig. 5 was obtained employing the prevaporized fuel configuration. It shows that ethyl propionate is easiest to ignite followed by methyl crotonate and methyl butanoate.

4 Comparison between Numerical Calculations and Experimental Data

Figures 6, 7, 8, and 9 compare experimental data with results obtained from numerical calculations using detailed chemistry. The fuel employed is methyl butanoate. In Figs. 6, 7, 8, and 9 the symbols are experimental data and the lines are results of numerical calculations. Figures 6 and 7 respectively show critical conditions of extinction and autoignition obtained employing the condensed fuel configuration of Fig. 1, while Figs. 8, and 9 show similar results obtained employing

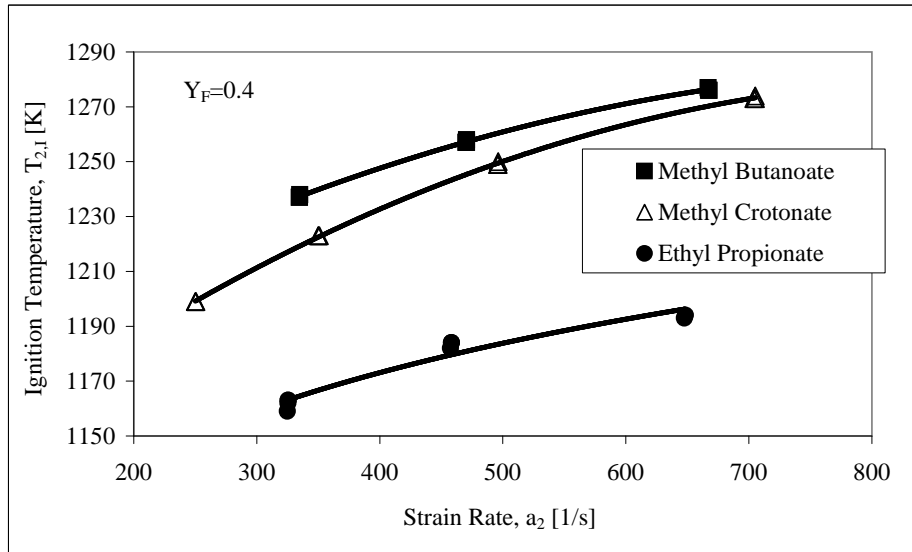


Figure 5: Experimental data showing the temperature of air at autoignition, $T_{0,I}$, as a function of the a_2 . The symbols represent measurements. The lines are best fits to the experimental data. The experimental data was obtained employing the prevaporized fuel configuration shown in Fig. 2

the prevaporized fuel configuration of Fig. 2. These figures show that the critical conditions of extinction and autoignition calculated using the detailed mechanism of Fisher et al [5] agree very well with experimental data.

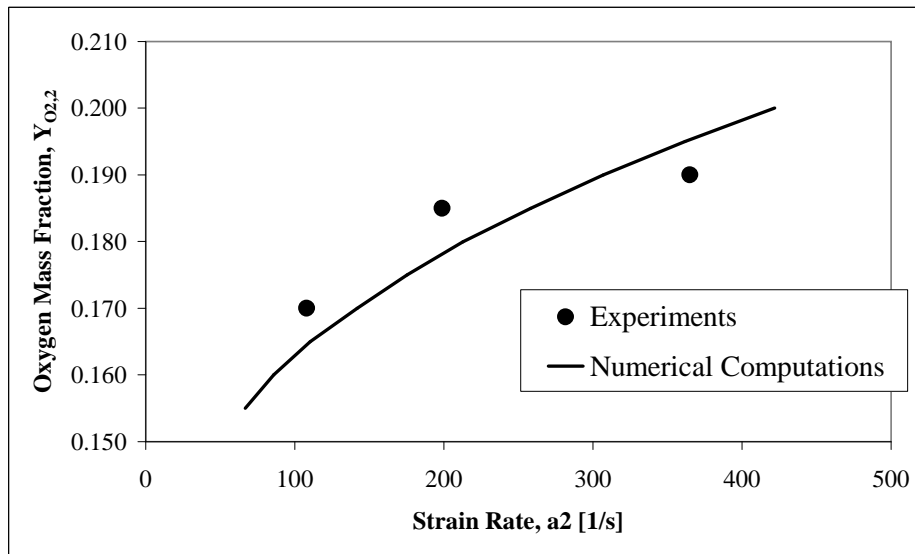


Figure 6: The mass fraction of oxygen in the oxidizer stream, $Y_{O_{2,2}}$, as a function of the strain rate, a_2 , at extinction. The fuel is methyl butanoate. The symbols represent measurements. The lines are results of numerical calculations. The experimental data and numerical calculations are obtained employing the condensed fuel configuration shown in Fig. 1

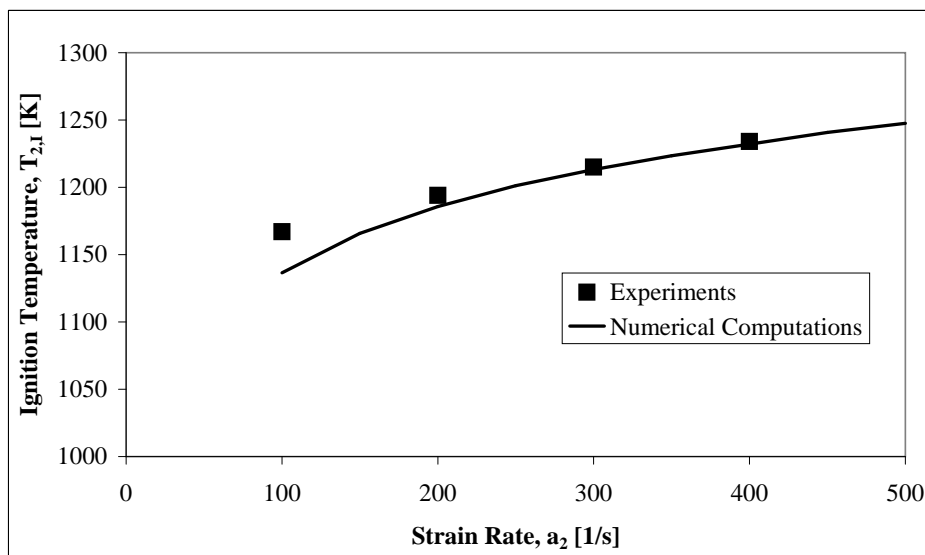


Figure 7: The temperature of air at autoignition, $T_{0,I}$, as a function of the strain rate. The fuel is methyl butanoate. The symbols represent measurements. The lines are results of numerical calculations. The experimental data and numerical calculations are obtained employing the condensed fuel configuration shown in Fig. 1

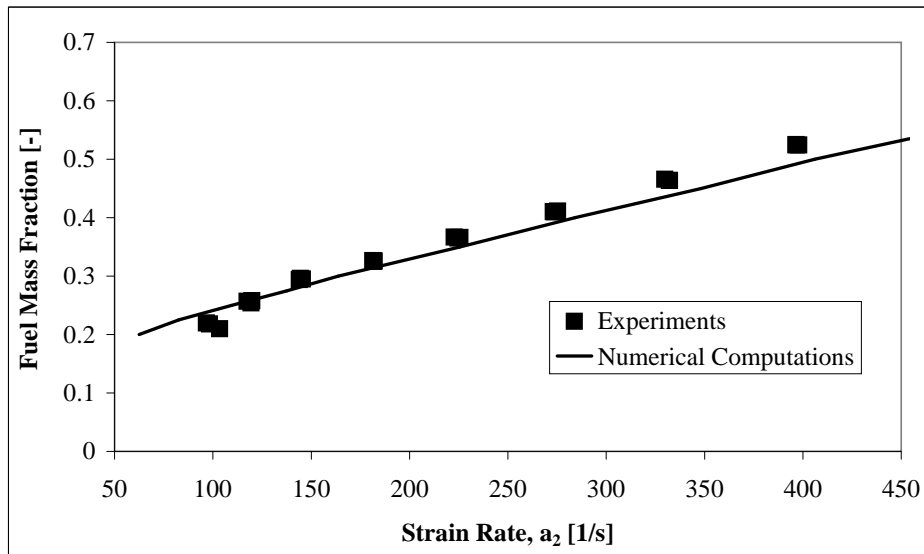


Figure 8: The mass fraction of fuel in the fuel stream, $Y_{F,1}$, as a function of the strain rate, a_2 , at extinction. The fuel is methyl butanoate. The symbols represent measurements. The lines are results of numerical calculations. The experimental data and numerical calculations are obtained employing the prevaporized fuel configuration shown in Fig. 2.

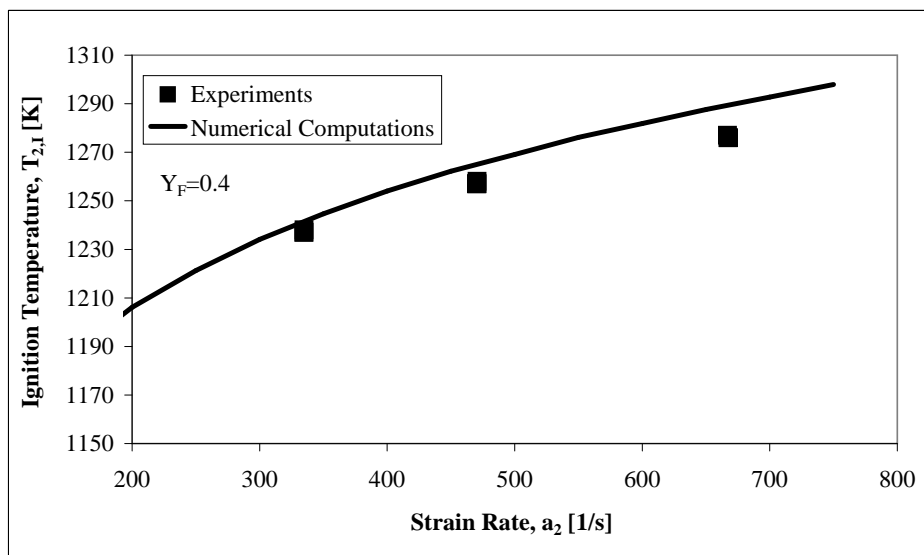


Figure 9: The temperature of air at autoignition, $T_{0,1}$, as a function of the a_2 . The symbols represent measurements. The lines are results of numerical calculations. The fuel is methyl butanoate. The experimental data and numerical calculations are obtained employing the prevaporized fuel configuration shown in Fig. 2.

Acknowledgments

The authors thank Dr. William Pitz at Lawrence Livermore Laboratories, Livermore, California for providing the chemical kinetic mechanism for methyl butanoate.

References

- [1] S. Fernando, C. Hall, and S. Jha. *Energy & Fuels*, 20 (2006) 376–382.
- [2] T. Pramanik and S. Tripathi. *Hydrocarbon Processing*, 84 (2005) 40–54.
- [3] M. S. Graboski, R. L. McCormick, T. L. Alleman, and A. M. Herring. The effect of biodiesel composition on engine emissions from a DDC series 60 diesel engine. Final Report NREL/SR-510-31461, National Renewable Energy Laboratory, Golden Colorado, 2003.
- [4] W. G. Wang, D. W. Lyons, N. N. Clark, M. Gautam, and P. M. Norton. *Environmental Science and Technology*, 34 (2000) 933–939.
- [5] E. M. Fisher, W. J. Pitz, H. J. Curran, and C. K. Westbrook. *Proceedings of the Combustion Institute*, 28 (2000) 1579–1586.
- [6] K. Seshadri and F. A. Williams. *International Journal of Heat and Mass Transfer*, 21 (1978) 251–253.
- [7] R. Seiser, K. Seshadri, E. Piskernik, and A. Liñán. *Combustion and Flame*, 122 (2000) 339–349.
- [8] H. Pitsch. Entwicklung eines Programmpaketes zur Berechnung eindimensionaler Flammen am Beispiel einer Gegenstromdiffusionsflamme. Master's thesis, RWTH Aachen, Germany, 1993.